Check for updates

Received: 13 October 2020 | Revised: 25 October 2021 | Accepted: 11 November 2021

DOI: 10.1002/cne.25278

JCN RESEARCH IN SYSTEMS NEUROSCIENCE THE JOURNAL OF COMPARATIVE NEUROLOGY WILEY

RESEARCH ARTICLE

The pigment-dispersing factor neuronal network systematically grows in developing honey bees

Katharina Beer[1] | Stephan Härtel[2] | Charlotte Helfrich-Förster[1]

[1] Department of Neurobiology and Genetics, Biocenter, University of Würzburg, Würzburg, Germany

[2] Department of Animal Ecology and Tropical Biology, Biocenter, University of Würzburg, Würzburg, Germany

Correspondence
Katharina Beer, Department of Neurobiology and Genetics, Biocenter, University of Würzburg, 97074 Würzburg, Germany.
Email: Katharina.beer@uni-wuerzburg.de

Funding information
German Research Foundation CRC 1047 "Insect Timing"; German Excellence Initiative to the Graduate School of Life Sciences, University of Würzburg; SCIENTIA, University of Würzburg

Abstract

The neuropeptide pigment-dispersing factor (PDF) plays a prominent role in the circadian clock of many insects including honey bees. In the honey bee brain, PDF is expressed in about 15 clock neurons per hemisphere that lie between the central brain and the optic lobes. As in other insects, the bee PDF neurons form wide arborizations in the brain, but certain differences are evident. For example, they arborize only sparsely in the accessory medulla (AME), which serves as important communication center of the circadian clock in cockroaches and flies. Furthermore, all bee PDF neurons cluster together, which makes it impossible to distinguish individual projections. Here, we investigated the developing bee PDF network and found that the first three PDF neurons arise in the third larval instar and form a dense network of varicose fibers at the base of the developing medulla that strongly resembles the AME of hemimetabolous insects. In addition, they send faint fibers toward the lateral superior protocerebrum. In last larval instar, PDF cells with larger somata appear and send fibers toward the distal medulla and the medial protocerebrum. In the dorsal part of the medulla serpentine layer, a small PDF knot evolves from which PDF fibers extend ventrally. This knot disappears during metamorphosis and the varicose arborizations in the putative AME become fainter. Instead, a new strongly stained PDF fiber hub appears in front of the lobula. Simultaneously, the number of PDF neurons increases and the PDF neuronal network in the brain gets continuously more complex.

KEYWORDS
Apis mellifera, circadian clock, immunohistochemistry, larval and pupal development, neuroanatomy

1 | INTRODUCTION

The circadian clock enables animals to anticipate the daily environmental changes on our planet and to adjust their behavior in daily activity and sleeping, including foraging rhythms. Honey bees have a most remarkable time memory, which they use to associate the location of a flowering resource to the daytime, when the plant opens its flower (Beling, 1929; Bloch et al., 2017). In their waggle dance, honey bee foragers communicate this location in relation to the sun to their nest mates, for which they have to compensate for the past time during flight (von Frisch, 1967). The circadian clock is involved in these complex behaviors of the honey bee, but the regulatory mechanism is largely unknown (Cheeseman et al., 2012; Jain & Brockmann, 2018).

This is an open access article under the terms of the Creative Commons Attribution License, which permits use, distribution and reproduction in any medium, provided the original work is properly cited.
© 2021 The Authors. *The Journal of Comparative Neurology* published by Wiley Periodicals LLC

In general, the clock gets synchronizing input signals from the environment like daily oscillations in sunlight or temperature. These signals are transmitted to the brain clock, where a transcriptional/translational feedback loop creates circadian oscillations in clock gene expression, which drive then rhythmic behavior and physiological processes (Dunlap, 1999). In most studied insects, clock gene expression is found in defined soma groups (pacemaker centers) located to the lateral and/or dorsal brain; for example in flies, bugs, bees and moths (Fuchikawa et al., 2017; Helfrich-Förster et al., 1998; Ikeno et al., 2014; Kobelková et al., 2015; Nässel et al., 1993; Vafopoulou et al., 2009; Weiss et al., 2009; Wise et al., 2002; Závodská et al., 2003). The first documentation of a light-dependent pacemaker center in the insect brain was by lesion studies in Madeira cockroach brains (Nishiitsutsuji-Uwo & Pittendrigh, 1968). Further transplantation studies in the Madeira cockroach located the pacemaker center to the optic lobes (Page, 1982) and in specific to the accessory medulla (AME) (Reischig & Stengl, 2003a). Neuronal organization and neurotransmitters in the AME of cockroaches show striking similarities to the suprachiasmatic nucleus, the circadian clock center in the mammalian brain (Homberg et al., 2003).

Homberg et al. (1991) recognized in a comparative study the potential of the neuropeptide pigment-dispersing factor (PDF) as an integrative part of the circadian clock in insects (reviewed in Homberg et al., 2003; Stengl & Homberg, 1994). The circadian clock is ubiquitous among insects and with genetic manipulation tools in the honey bee still largely missing, comparative anatomical studies provide a good way to elucidate pathways that are involved in generation of clock regulated behavior (Beer & Helfrich-Förster, 2020a). Indeed, PDF is a highly conserved clock component in panarthropods (Iga, 2016; Martin et al., 2020; Mayer et al., 2015; Shafer & Yao, 2014). This neuropeptide regulates rhythmic behavior, for example, daily activity-rest cycles in cockroaches or flies (Petri & Stengl, 1997; Renn et al., 1999; reviewed in Helfrich-Förster et al., 2011), but was also shown to be involved in receiving the environmental light input signals to the clock of cockroaches (Petri et al., 1995; Schendzielorz & Stengl, 2014; reviewed in Helfrich-Förster, 2020). In addition, it is a major communication factor between different clock cells in the insect brain (Im & Taghert, 2010; Lin et al., 2004; Schneider & Stengl, 2005; Tomioka et al., 2008; Yao & Shafer, 2014). Furthermore, it regulates physiological processes, for example, mating (Krupp et al., 2013) and renal function (Talsma et al., 2012) of flies. Though it is not esssential, PDF additionally seems to contribute to regulation of the normal rhythmic eclosion in fruit flies (Selcho et al., 2017; Helfrich-Förster et al., 2000). Also, in honey bees, it was demonstrated to be part of the circadian system (Beer et al., 2018; Fuchikawa et al., 2017). The central clock protein PERIOD is coexpressed in all PDF neurons (Fuchikawa et al., 2017), and injection of synthetic PDF peptide into the brain of adult bees can shift the activity phase in circadian rhythms in locomotion (Beer et al., 2018).

In various different insects, the cell bodies of PDF producing neurons (PDF neurons) are located in the lateral brain, send fibers into the AME, which is a small neuropil at the base of the medulla, as well as to different centers in the dorsal brain, the central brain and also to the optic lobe (Helfrich-Förster, 2005; Helfrich-Förster et al., 1998; Homberg et al., 1991). The PDF neuronal network in the honey bee is similarly organized, but the PDF neuron arborizations are numerous and highly complex, especially in the protocerebrum (Beer et al., 2018; Sumiyoshi et al., 2011). So far, it was not possible to track single PDF neurons in honey bee brains to its projection destination and gather conclusions on their function. For example, in flies, cockroaches and locusts, different subpopulations of PDF neurons have been identified (Homberg et al., 1991; Nässel et al., 1991, 1993). The large ventrolateral neurons of *Drosophila* project contralaterally to the other hemisphere and are involved in the light-input pathway of the circadian clock, while the small ventro-lateral neurons arborize within the hemisphere and are most important for generating circadian rhythms in locomotion (Helfrich-Förster, 2020; Klose et al., 2016; Schlichting et al., 2016). In the cockroach, PDF neurons are grouped in four soma clusters: two lie in the lamina, one in the posterior cell cortex of the medulla and one close to the AME; the AME neurons were categorized in three size groups and also in different groups according to their signaling properties (Gestrich et al., 2018; Petri et al., 1995; Reischig & Stengl, 2003b; Wei et al., 2010, 2014). Four contralaterally projecting PDF neurons of the AME are major contributors to the circadian rhythms in locomotion (Soehler et al., 2011). In the honey bee, no PDF neurons are present in the lamina and posterior medulla. All ~15 PDF neurons cluster together anteriorly of the AME, but we noticed that they differ in size and could often see one PDF neuron with large soma that was located most anteriorly, suggesting that the PDF neurons form several subpopulations within this cluster (Beer et al., 2018). Another peculiarity of the bee was that arborizations in the AME were not very prominent, and the densest concentration of PDF fibers was found anterior of the lobula (Beer et al., 2018). A respective PDF-neuropil was also found in the Madeira cockroach (Fleissner et al., 2001; Wei et al., 2010).

Here, we analyzed for the first time the PDF neuronal network of honey bees of different developmental stages raised under laboratory conditions in order to assess the anatomy and putative function of individual (or subgroups) of PDF neurons in the honey bee clock. To do so, we performed anti-β-pigment-dispersing hormone (PDH) immunostaining in larvae and pupae of *Apis mellifera*. This antibody was specifically raised against synthetic crab PDH (Dircksen et al., 1987), but has been shown to recognize PDF in the nervous system of insects including honey bees (Beer et al., 2018; Fuchikawa et al., 2017; Helfrich-Förster, 1997; Homberg et al., 1991; Nässel et al., 1993; Park & Hall, 1998; Petri et al., 1995; Rao & Riehm, 1993; Sehadová et al., 2004; Stengl & Homberg, 1994; Sumiyoshi et al., 2011; Závodská et al., 2003). The anti-β-PDH does also recognize PDFs from mollusks, nematodes, onychophores and tardigrades (Elekes & Nässel, 1999; Iga, 2016; Janssen et al., 2009; Martin et al., 2020; Mayer et al., 2015) showing that PDF/PDH peptides have evolved before Cycloneuralia and Panarthropoda have separated, although data are still missing from Loricifera, Kinorhyncha and Nematomorpha (Mayer et al., 2015). Only in crustacea, these peptides are called PDHs. For the sake of simplicity, we will call the β-PDH-immunoreactive neurons in the honey bee brain "PDF neurons" throughout this study.

Studying the development of the PDF network should reveal whether there are subgroups of PDF neurons in honey bees as there are in other insects and if so, where they project to. For example, in holometabolous fruit flies, only the four PDF neurons with small

somata (small ventro-lateral neurons) can be seen in larval brains (Helfrich-Förster, 1997). These neurons send dendrites to the larval optic neuropil, which receives input from the larval eyes and develops into the AME during metamorphosis (Helfrich-Förster et al., 2002). Furthermore, the larval PDF neurons project into the dorsal protocerebrum where they terminate anteriorly and ventrally of the calyces of the mushroom bodies. At about 50% of pupal development, the four further neurons with large somata (large ventro-lateral neurons) start to express PDF. These invade the developing AME and additionally the optic lobes.

In contrast to flies and cockroaches, bee larvae are rather immobile and do not need to search for food since they are fed by nurses. They possess no photoreceptor organs (larval stemmata and ocelli) and are therefore blind (Gilbert, 1994). Hence, it is unknown whether they possess a larval optic neuropil. It is also unknown how the AME develops in the honey bee brain and which relation it has with the PDF neurons. Here, we describe similarities and differences of the developing PDF fiber network between honey bees and the so far best studied insects, the Madeira cockroach and the fruit fly.

2 | MATERIALS

2.1 | Honey bees

Honey bee colonies, species *A. mellifera*, subspecies *carnica*, were kept at Department of Animal Ecology and Tropical Biology, the University of Würzburg. Queens were inseminated by multiple drones. Standard beekeeping methods were applied with bees kept in field colonies consisting of ~35,000–40,000 bees.

3 | METHODS

Insect brain tissues of different developmental stages in the honey bees were stained via immunofluorescence, and the neuronal network was additionally 3D reconstructed to visualize the development of the clock neuronal network. We removed dead bees and performed feeding and sampling always at the same time of the day (resembling the subjective morning at approximately ZT0), and the bees were otherwise undisturbed in the incubator.

3.1 | In vitro rearing of honey bee larvae

In order to standardize sample taking of different developmental stages of honey bees, we reared the larvae in vitro (for detailed method explanation see Aupinel et al., 2005, 2007; Hendriksma et al., 2011; Steijven et al., 2017). We caged a queen overnight on an empty brood comb, and 3 days later first instar larvae were grafted into artificial rearing cells (Cupularve Nicotplast, Maisod, France) in 48-well plates that were loaded with preheated larval diet (35°C) (for dietary plan see Table 1). The well plates were sanitized with cotton rolls soaked in 0.4% antimicrobial methylbenzethonium chloride glycerol solution (84.5% and 15.5%) and kept at 35°C ± 0.1°C and 97 ± 10% room temperature (RH) in a rearing chamber (Memmert, loading model 100–800, Schwabach, Germany). With this method, approximately 80–90% of the grafted larvae pupated and approximately 50% emerged as adult bees. For feeding and sampling, we placed the plates on a heating plate (35°C). We sampled larval instars L1, L3 and L5 (determined by age, see also Hendriksma et al., 2011) and different pupal stages P1, P3, P5, P7 and P9 (determined by age and morphology according to Groh & Rössler, 2008). P1 were white eyed with white body, P3 orange/pink eyed with white body and P5 were red-brown eyed and already showed cuticle tanning of the first two leg pairs and yellow head and thorax. In P7, the bees had light brown bodies with speckled legs and folded grey wings. On the day before emergence, bees entered the last pupal stage (P9) and appeared already adult-like with dark grey thorax and unfolded wings, but they were largely motionless.

TABLE 1 Timetable for feeding and sampling larval instars during in vitro rearing

	Day 1	Day 2	Day 3	Day 4	Day 5	Day 6
Diet amount	20 µl		20 µl	30 µl	40 µl	50 µl
Development	**L1**–L2	L2–L3	**L3**–L4	L4–L5	**L5**	L5

Notes: Feeding protocol started on day 1 when larvae were grafted into artificial rearing cells. Diet composition and amount changed with age (see for details Aupinel et al., 2005). We changed the protocol slightly and applied diet of days 1 and 2 on the first day together. The corresponding development of the bees (L1–5: larval instar 1–5) is indicated below. We sampled instar L1, L3 and L5 on the morning of days 1, 3 and 5, respectively (indicated by bold letters).

3.2 | Immunostaining PDF neurons in larvae brains

We prefixed the larval tissue after poking holes with a sharp needle into the larvae for 5 h in 4% paraformaldehyde (PFA) and phosphate buffered saline with 0.1% Triton (0.1%) (PBST) at (RT) of 20°C–22°C, washed three times in PBS (each 10 min) and dissected the brains using forceps with slightly curved tips in PBS. Afterward, we fixed the brains a second time for 1 h at RT. We added the second fixation of the dissected larvae brains because in preliminary experiments, we lost occasionally brains due to tissue solving in the washing steps. The results of these preliminary larval staining experiments were nonetheless comparable to those, we present here. In experiments with bee larvae, no shaker was used except in the first fixation step because larval brain tissue is extremely delicate. Fixed brains were washed (three times in PBS and three times in PBST [0.5%]) and preincubated in 5% NGS-PBST (0.5%) at 4°C overnight. The brains were then incubated in 1:3000 anti-β- PDH antibody solution (in 5% NGS-PBST [0.5%] and 0.02% NaN_3) for 3 days at 4°C and 1 day at RT. The affinity-purified rabbit antiserum against β-PDH was provided by Dr. Heinrich Dircksen (University of Stockholm, Sweden). This polyclonal anti-β-PDH antibody was raised against *Uca pugilator/Cancer magister* PDH (NSELINSILGLPKVMNDAa) and bovine thyroglobulin

(Dircksen et al., 1987) and in a specificity test with preincubation of diluted PDH antibody on 10 μM *Uca pugilator/Cancer magister* β-PDH peptide, all immunoreactive staining in cockroach brains was abolished (Stengl & Homberg, 1994). Other studies used this antibody to immunostain the PDF peptide in various insects, including hymenoptera (Beer et al., 2018; Bloch et al., 2003; Fuchikawa et al., 2017; Kay et al., 2018; Weiss et al., 2009). Antibody specificity seems to be true also for *A. mellifera* because recent staining experiments with the anti-β-PDH (Beer et al., 2018; Fuchikawa et al., 2017) and an anti-*am*-PDF (Sumiyoshi et al., 2011) antibody produce highly similar results. The brains were washed six times in PBST (0.5%), incubated in the secondary antibody solution (1:200 Alexa Flour 635 goat antirabbit in 5% NGS-PBST [0.5%]) and then washed again (three times in PBST (0.5%) and three times in PBS) before we mounted them in mounting medium for fluorescence (Vectashield, Vector laboratories, CA, USA). Some of the larval brains were mounted between microscope cover slides with spacers. Only these larval brains were used for analysis of cell size and staining intensity of PDH immunoreactive neurons because we wanted to treat the larvae brains and pupae brains exactly the same for these quantification analyses.

3.3 | Additional antihorseradish peroxidase staining

In some of the larvae and pupae, we additionally immunostained the developing neuropils and somata of the neurons with antihorseradish peroxidase (HRP) antibody, which recognizes a carbohydrate residue of the neuron-specific cell surface protein Nervana (nerve antigen) in the insect nervous system (Sun & Salvaterra, 1995). For the anti-HRP staining, we imbedded the pupae brains in 6% agarose (Hydroxyethylagarose CAS No. 39346-81-1, Carl Roth Gmbh + Co. KG, Karlsruhe, Germany) and produced 90 μm thick vibratome slices (speed and frequency at medium settings; Leica VT1000 S vibrating blade microtome, Leica Microsystems, Wetzlar, Germany). We incubated the brains with Cy3-AffiniPure Goat Anti-HRP (catalog No. 123-165-021, Jackson ImmunoResearch, West Grove, PA, USA) diluted at 1:300 in PBST 0.5% (with 5% NGS and 0.02% NaN3) for 48 h at RT and washed five times in PBST (0.5%) and three times in PBS. Afterward, the larval brains were mounted between microscope cover slides with spacers in mounting medium for fluorescence. Sectioned pupae brains were mounted on microscope slides.

3.4 | Immunostaining clock neurons in pupae brains

The staining procedure for pupae bee brains was very similar to the staining procedure in larvae brains, and we adjusted it only for a few steps. Bees were decapitated and a window was cut into the cuticle of the frontal head. This procedure took only a few minutes. Heads were then fixed in 4% PFA in PBST (0.1% Triton) for 3–4 h on a shaker. All washing and incubation steps were performed on a shaker. After washing the heads in PBS three times (10 min each), brains were dissected in PBS and washed again three times in PBS. Brains were incubated in sodium citrate buffer (10 mM, pH 8.5) at 80°C in an antigen retrieval step. Afterward, we washed the brains 10 times in PBS, two times in PBST (0.5%), one time in PBST (2%) and one time in PBST (0.5%). The following steps of washing and antibody incubation were performed as described above for the larvae brains with the difference that primary antibody incubation time was increased to 6 days at 4°C and 1 day at RT. We mounted the brains between two microscope cover glasses with spacers in mounting medium for fluorescence, which prevented the tissue from being crushed. The spacers were self-made by stacking eight customary hole reinforcements. We also immunostained PDF in some sectioned brains (for vibratome sectioning procedure see HRP staining). Sectioned brains were incubated for 2 days in PDH antibody solution at RT. The following steps were performed like in whole mount preparations. Sectioned pupae brains were mounted on microscope slides, but excluded from the cell size analysis for sake of consistency across experiments.

3.5 | Data analysis

Immunocytochemistry data were analyzed with a Leica TCS SPE confocal microscope (Leica Microsystems, Wetzlar, Germany) equipped with 10×/0.30 CS ACS APO and 20×/0.60 IMM CORR ACS APO objectives. Brains were scanned sequentially in stacks (Leica Application Suite Advanced Fluorescence 2.7.3.9723, Leica Microsystems). Samples of one experiment were processed with the same settings, and obtained confocal pictures (resolution 1024 × 1024) were further processed in Fiji ImageJ (version 1.49, Wayne Rasband, National Institutes of Health, USA) and in Corel Photopaint (Corel Corporation 2018). We counted PDF immunoreactive neurons in 157 brains of differently aged developing honey bees and measured size, staining intensity and relative location in the brain of over 2000 cell bodies. Some of the larvae brains were mounted on microscope slides without spacers to optimize fluorescence detection. These brains were not used for quantification of cell size, staining intensity and cell body location in the brain because we wanted to compare here only brains treated exactly the same in order to standardize across experiments. Quantification of cell number was done by counting stained cells in both hemispheres and then averaging for the brain. In order to judge whether there are different subpopulations of PDH immunoreactive neurons, we investigated possible differences in staining intensity and location of the somata in relation to the cell body size. Average staining intensity was measured for the area of the whole cell bodies at the plane, which showed the middle of the nucleus, and background staining in the area of the nucleus was subtracted. The same plane represents the largest expanse of the cell body, which was used for quantification of cell body size. Since brains were mounted on different slides, we measured location of the PDH immunoreactive cell bodies via number of scanning steps in the frontal confocal scans in which the cell bodies are visible. Afterward, we ranked them from 1 (most posterior) to 16 (most anterior) in pupal stages. In L3, ranking was from 1 to 6 and in L5 from 1 to 8. We

compared staining intensity and relative cell body location with cell body size separately for larvae and pupae because the overall brain structure of larvae and pupae differed. Additionally, complexity of the network of PDH immunoreactive neurons was quantified via counting neuronal fibers in predefined areas in brains of bees in pupal stage P1 and P9. This analysis was only possible for certain fiber tracts in which individual PDF fibers were discernable. For this purpose, we defined a plane in the middle of the region we chose for quantification and counted the fibers crossing this plane perpendicular. Subsequently, brightness, intensity and contrast were adjusted in the figures displayed in the results section. Statistical analysis and graphs were made with R (R version 3.6.1, packages stats and ggplot2). None of the data sets were normally distributed (Shapiro–Wilk normality test). The cell size data were therefore analyzed by the Kruskal Wallis test followed by a Wilcoxon rank sum test for post hoc pairwise comparison. We tested for differences between fiber numbers in P1 and P9 pupal stages with Wilcoxon rank sum test with continuity correction. To investigate correlation of cell size with staining intensity and position in the brain, we used Kendall's rank correlation test.

3.6 | Nomenclature

We used the nomenclature of Ito et al. (2014) to describe structures in the bee brain. For simplicity, developing structures in the larval brain were named like in adult insect brains. For PDF specific tracts, we referred to the PDF network described in detail for the cockroach (Giese et al., 2018; Wei et al., 2010). The PDF fiber network in honey bees displays in some areas a more complex structure with many rather densely bundled fibers, but overall network organization is similar. For comparison with the PDF arborization network in the adult honey bee brain, we refer to Beer et al. (2018).

4 | RESULTS

4.1 | Larval instars

The honey bee has five larval instars during which the blind larvae are fed by the nurses and increase dramatically in size. As in other holometabolic insects, their compound eyes develop only during metamorphosis; therefore, their optic lobe primordia are barely developed in the first two larval instars (Marco Antonio & Hartfelder, 2017). We could detect the precursor of the medulla and about three PDF neurons per hemisphere for the first time in the optic lobe primordia of third larval instars (L3) (Figure 1). The somata of the PDF neurons (3.1 ± 0.4, mean ± STE, n = 29) were located in the anterior cell body rind ventrally to the developing medulla (arrow heads in Figure 1a–d). The neurites of the PDF neurons follow fibers of putative medulla cortex neurons that are stained by anti-HRP and run dorsally to the base of the developing medulla (thin arrows in Figure 1a,c). The neurites of all developing medulla neurons converge at the dorsally located base of the medulla (asterisk in Figure 1d,f,g), giving the developing medulla the shape of an asymmetric fan of HRP-positive fibers (Figure 1d). The handle of the fan consists of fibers that leave the medulla and project to the protocerebrum of the central brain (Figure 1d,g). The PDF-positive neurites form a dense varicose fiber network at the base of the medulla, while weakly stained PDF fibers follow the HRP-stained medulla neurons to the protocerebrum (Figure 1c,d,f,g). These terminate in the ipsilateral superior protocerebrum (Figure 1g). It was not possible to trace single PDF neurons because all the neurites of all three PDF neurons fasciculated with each other and intermingled in the dense fiber network (asterisks in Figure 1a,c,e). The dense PDF fiber network at the base of the medulla resembles from its position the larval optic neuropil of fruit fly larva (Helfrich-Förster et al., 2002) and from position and structure the AME of hemimetabolous insects (Homberg et al., 1991; Homberg & Prakash, 1996; Wei et al., 2010). Since there are no larval eyes that can innervate this neuropil, we are reluctant to call it larval optic neuropil and will talk about AME-like structures in the following.

In L5 larvae, the projections of the PDF neurons into the lateral protocerebrum via the lobula valley tract (LVT) became more prominent revealing that they terminate ventrally to the developing mushroom bodies (Figure 2a,c). Furthermore, in late L5 larvae, the projections bifurcated in the superior and lateral protocerebrum into two thin fibers of which one ran toward the mushroom bodies and the second toward the medial protocerebrum (Figure 2d). In L5 larvae, approximately six PDF neurons (5.6 ± 0.3, mean ± STE; $n = 38$) per hemisphere were present (see Figure 4), and their projections did not only extend toward the medial protocerebrum but also distally from the AME-like structure to the future serpentine layer of the medulla, which separates the proximal and distal medulla in the adult brain (Figure 2a–e). The PDF-positive neurites seem to follow outgrowing HRP-positive fibers from the proximal to the distal medulla that enter the serpentine layer at a defined point in its upper third (arrows and small open circles in Figure 2). The PDF-positive fibers formed a kind of knot at this entry point, and then started to grow first in ventral and later also in dorsal direction along the developing serpentine layer. Again, we could not see whether all of the neurons or just some of them projected toward the medial protocerebrum and the distal medulla because the projections were already densely packed in the tract running toward the AME-like structure, which made single tracing of neurites impossible. Nevertheless, in L5, for the first time, PDF neurons with larger somata appeared and especially one large soma was conspicuous because it was at least by 10 μm^2 larger than the other cells in the cluster. We detected this large neuron in 32% of all analyzed hemispheres ($n = 38$), and in half of the cases it was located in an anterior position in the PDF–cell cluster. The appearance of large PDF neurons nicely correlated with the appearance of PDF projections toward the distal medulla and the medial protocerebrum, suggesting that a new set of PDF neurons was born in the fifth and last larval instar of the honey bee. In none of the L5 brains, we could see any PDF fibers running into the developing lamina. At this stage, the future lamina emerges as an upfolding in the outer optic lobe anlagen, but still makes no connection to the medulla (Marco Antonio & Hartfelder, 2017). Since HRP labels only neurons and not neuroblasts, we could not detect any HRP labeling in the future

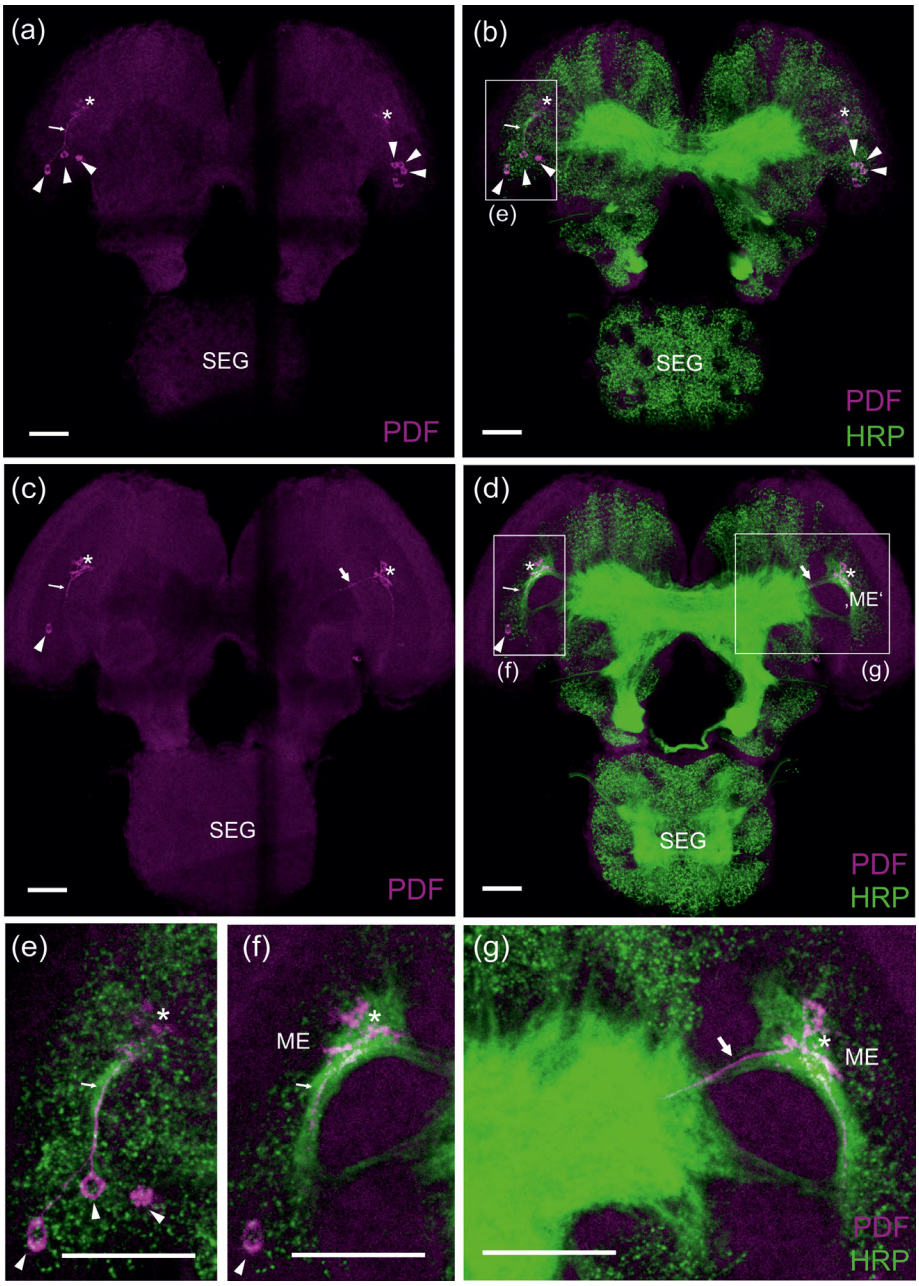

FIGURE 1 Pigment-dispersing factor immunoreactive neurons (PDF neurons) and fibers (magenta) in the brain of third larval instars. All images are projections of 10 confocal images (*z*-stack step size: 2.5 μm, pixel size: 0.36 μm) of whole mount brains. To visualize the developing neurons, the brain was costained with an antibody against horse-radish peroxidase (HRP) that labels the neuronal specific cell surface protein Nervana (green). Note that this antibody stains only neurons and not neuroblasts. The latter are much larger than neurons and can be seen as regular "empty holes" that are surrounded by neurons in the subesophageal ganglion (SEG) in (b). (a–d) Frontal overviews of the entire brain from anterior (a), (b) and from more posterior (c), (d). Arrow heads point to the somata of the PDF neurons, thin arrows to their projections to an "accessory medulla" (AME)-like structure (marked by asterisks), and the thick arrows indicate fibers that leave the AME-like structure toward the central brain. (e–g) Magnifications of the areas shown in (b) and (d) to show that the PDF-positive neurites follow major fiber tracts of other medulla (ME) neurons. Scale bars: 50 µm

lamina, confirming that neurogenesis has not yet started (Figure 2). At the end of L5, the late cocoon spinning phase, the first ommatidial cartridges of the retina appear and the photoreceptor axons start to grow toward the lamina (Marco Antonio & Hartfelder, 2017) (Figure 3a,b). We still could not see any HRP labeling in the prospective lamina, but we detected the first columnar structures in the developing distal medulla (Figure 3b,c)). At this stage, the arborizations of the PDF neurons in the serpentine layer became prominent, and this was especially true for the small knot at their entry point (Figure 3b–d).

The fifth instar ends with the larvae entering the prepupal stage, a stage characterized by profound metamorphic changes, such as the appearance of pupal head structures and a constriction separating the

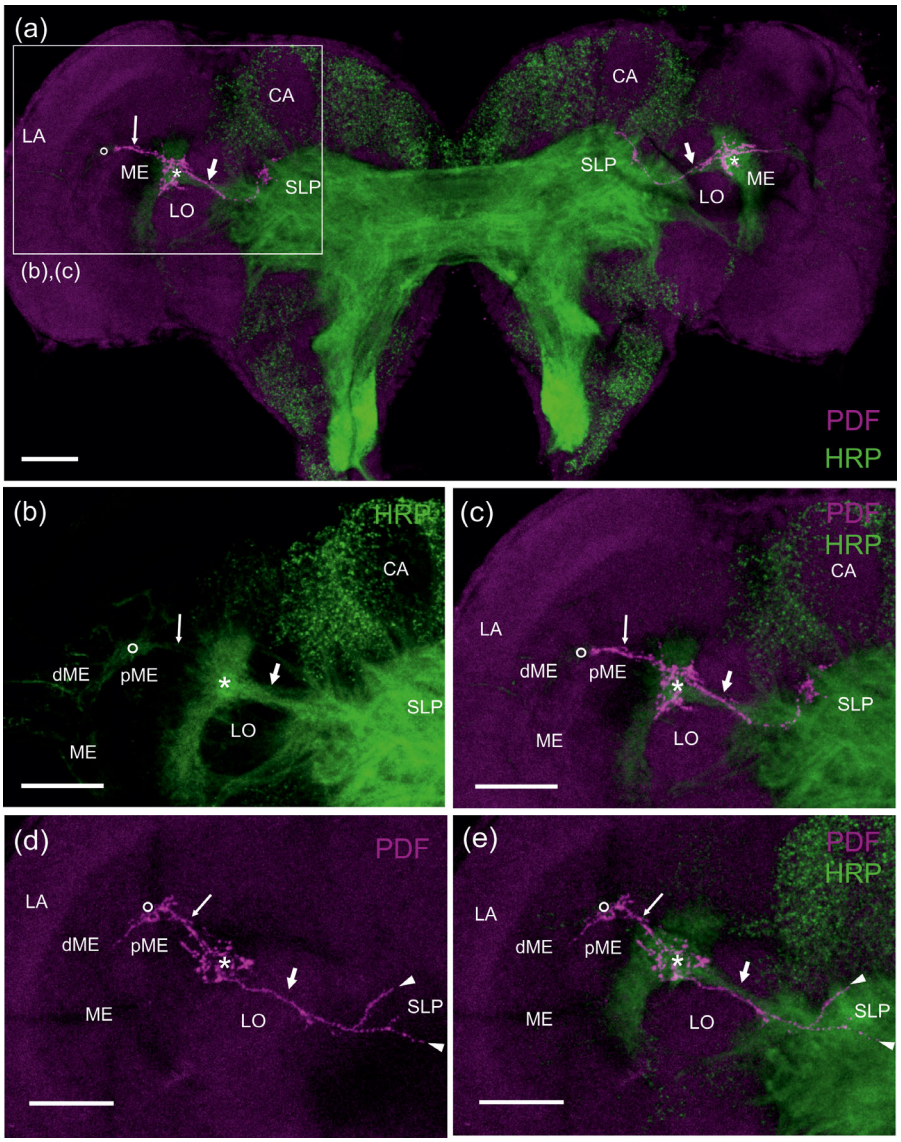

FIGURE 2 Pigment-dispersing factor (PDF) fibers in the brain of early fifth larval instars. All images are projections of 10 confocal images (*z*-stack step size: 2.5 μm, pixel size: 0.54 μm) of whole mount brains. Labeling is the same as in Figure 1. (a) Frontal overview of the brain without subesophageal ganglion. The somata of the PDF neurons are not included in this confocal stack. The PDF neurons project into the accessory medulla (AME)-like structure (asterisks) and from there distally to a knot (circle) in the serpentine layer of the medulla and medially toward the superior lateral protocerebrum (SLP) where they terminate lateral and ventral of the calyces (CA) of the mushroom bodies. Here only the lateral calyx (CA) is visible. (b and c) Magnifications of the indicated area in (a), only marked by antihorseradish peroxidase (HRP) and with both stainings overlayed (c) to visualize that the PDF fibers follow again the projections of other neurons. (d and e) The same brain area as shown in (b), (c), but from a slightly older fifth larval instar. The two arrow heads indicate that additional to PDF fibers that terminate ventrally of the calyces, a second fiber that invades more medial brain areas split off. Otherwise, same labeling as in the other panels. Abbreviations: CA, developing Calyx; dME, developing distal medulla; LA, developing lamina; LO, developing lobula; ME, developing medulla; pME, developing proximal medulla; SLP, superior lateral protocerebrum. Scale bars: 50 µm

thorax and abdomen. During this stage, the pupal cuticle is synthesized underneath the dissolving larval cuticle (Marco Antonio & Hartfelder, 2017). The animal is now in its prepupal stage during which it molts twice until it reaches the first pupal stage (P1), about 3 days after cell sealing (Groh & Rössler, 2008). Unfortunately, it was impossible to dissect the animals in the prepupal stages because all internal structures were rather fluid.

4.2 | Pupal stages

In the honey bee, nine pupal stages can be distinguished (Groh & Rössler, 2008). During these stages, eyes, optic lobes, antennal lobes and central protocerebral structures such as the mushroom bodies and central complex are already present and develop into their adult shape. The external structures such as the head, antennae, mouthparts,

thorax, legs and abdomen show adult-like characteristics already at pupal stage 1, but are still unpigmented.

The number of the PDF-positive somata and the complexity of the PDF-positive fiber network increased steadily during pupal development. Figure 4 shows the number and appearance of the PDF neurons throughout the entire development pooled from three different experiments that all yielded the same result. While the smaller cells had an almost round shape, the larger ones were usually oval (Figure 4a,c,d). The Kruskal Wallis test revealed a significant increase in the number of PDF-positive neurons throughout development (H: 138.87, $df = 7$, $p < .01$), and the post hoc pairwise comparison showed that the increase happened in three significant steps from their first appearance in L3. The first significant increase by ~3 neurons occurred from L3 to L5, the second by ~4 neurons from L5 to P1 and the third by ~3 neurons from P3 to P5 (Figure 4b). Not only the number of immunostained neurons increased, but also their staining intensity appeared to increase (compare Figure 4a and c). In addition, staining intensity was higher in large PDF somata as compared to smaller somata (see also Section 4.3). As in larval brains, we could also spot one (or occasionally two) very large PDF somata throughout the pupal stages. However, the frequency of their occurrence dropped to around 25%. As found for larvae, they were often located anterior in the PDF cell cluster in half of the cases. They are marked by an asterisk in Figure 4d. The smallest PDF cell bodies were usually located posterior in the

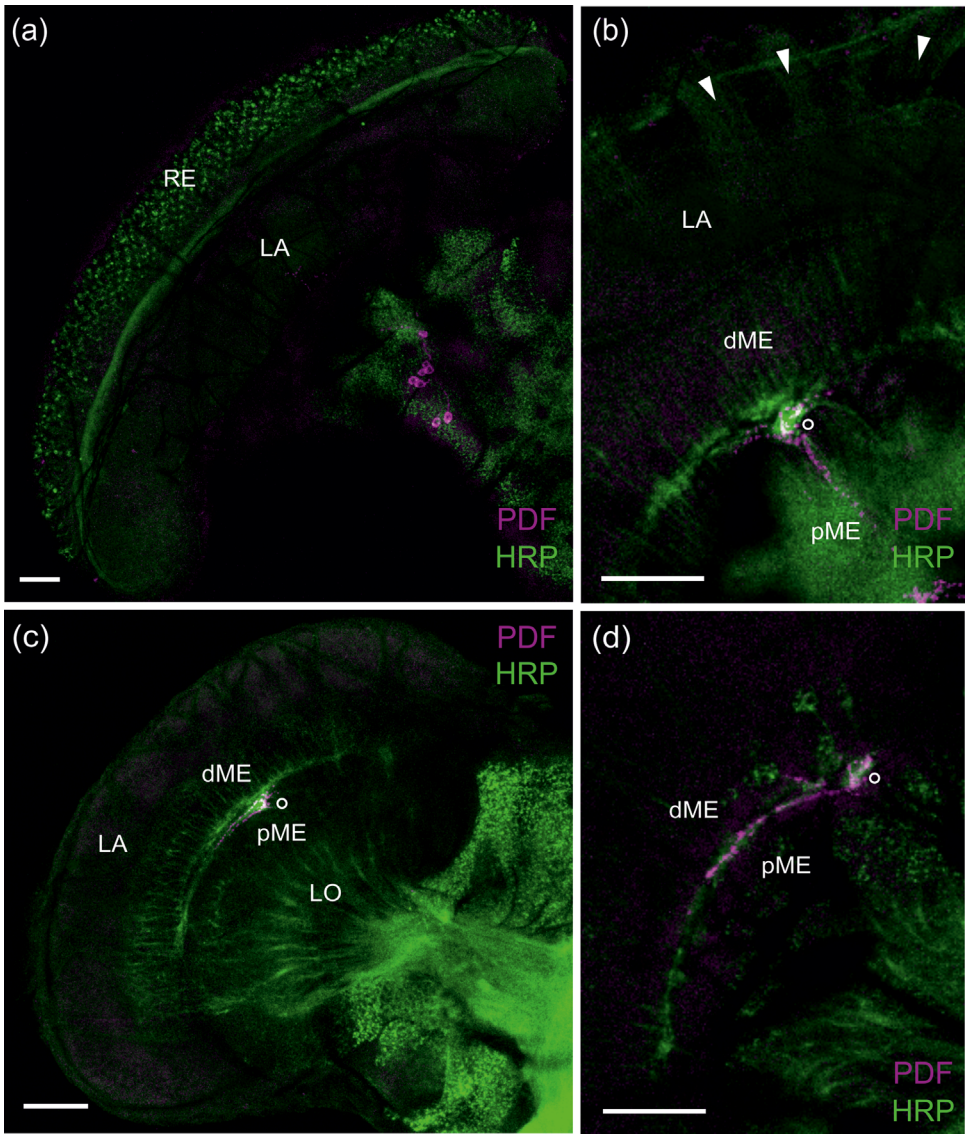

FIGURE 3 Pigment-dispersing factor (PDF) immunoreactive fibers in the brain of late fifth larval instars. All images are projections of 10 confocal images (z-stack step size: 2.5 μm, pixel size: 0.86 μm and 0.72 μm) of whole mount brains. Only the developing left optic lobe is shown. Labeling is the same as in Figure 1a,b,d: Images from the same brain from anterior (a) to posterior (b). (c) Image from another brain at the level of image (b). All images visualize the developing lamina (LA) that is not yet labeled by antihorseradish peroxidase (HRP), and the medulla (ME) that is labelled and shows the first subdivision in distal and proximal medulla (dME and pME). The retina is visible in (a) and starts to send its first projections to the lamina (arrow heads in [b]). The PDF fibers have reached the serpentine layer of the medulla that subdivides the proximal and distal medulla and enter it in a pronounced knot (circle). In the knot, the PDF fibers bifurcate and follow the serpentine layer ventrally (b–d) and dorsally (b). The lobula (LO) can be vaguely seen in (c). Scale bars: 50 µm

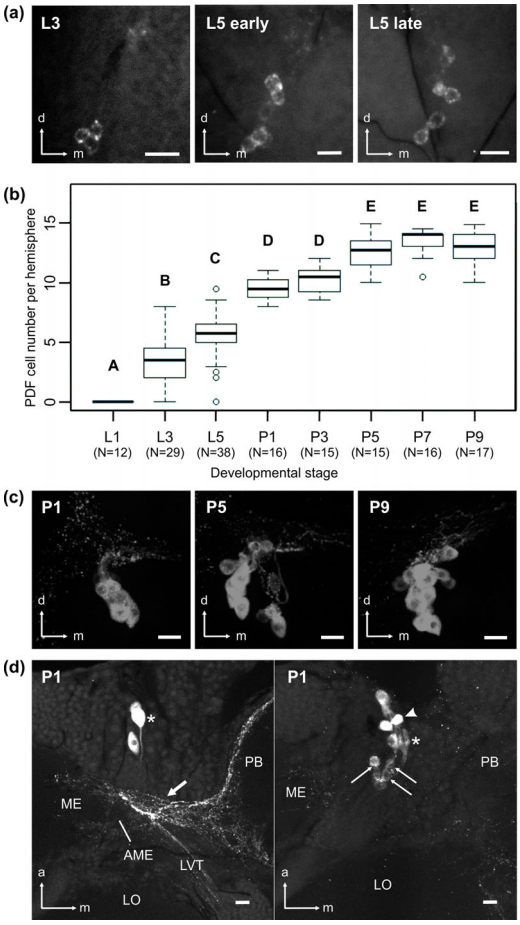

FIGURE 4 Number of pigment-dispersing factor (PDF) neurons throughout development and PDF somata in pupae. (a) Detail images of the PDF cell bodies in larval stages L3, and early and late L5 stage. The number of PDF neurons increases throughout development to build the highly complex clock neuron network of the adult honey bee (b). Different letters indicate statistically different groups (box plots; sample sizes are indicated with the sample group). (c) Detail images of the PDF cell bodies in the pupal stages P1, P5 and P9. (d) Projection images of PDF cell bodies and arborizations to the accessory medulla (AME)-like structure and toward the lateral protocerebrum (PB). Brain is slightly frontally tilted and sliced in a horizontal plane (vibratome slices). The left image shows the arborizations toward the AME-like structure and some of the bigger PDF cell bodies, which are slightly ventrally of the AME-like structure, but visible because of the frontally tilted position of the brain. The right image shows the following section, more ventrally located of the AME-like structure. Here, the other bigger PDH cell bodies are visible and most posterior within the cluster (and also closest to the AME-like structure) are three of four small PDF cell bodies located (arrows). Another small PDF cell body (marked with an arrow head) is located in the middle of the cluster. The two biggest PDF cell bodies (marked with asterisks) are located rather anterior (left image) and one in the middle of the cluster (right image). Images are frontal projections of confocal stack images (*z*-step size between images in (a) and (d) 2 μm; L3: 8 image stack (pixel size: 0.36 μm); early L5: 15 image stack (pixel size: 0.54 μm); late L5: 15 image stack (pixel size: 0.72 μm); scans in (d) left to right: 10 image stack (pixel size: 0.54 μm) and 22 image stack (pixel size: 0.54 μm); *z*-step size in (c) 1.5 μm and pixel size: 0.22 μm; P1: 55 image stack, P5: 63 image stack, P9: 41 image stack). Abbreviations: d, dorsal; m, medial; ME, medulla; LO, lobula. Scale bar: 20 µm

cluster (closer to the AME-like structure) (marked by arrows in Figure 4d) and had a rather roundish shape compared to the oval shaped big PDF cell bodies.

In parallel to the increase in PDF neuron number, also their arborization network in the central brain and the optic lobes increased. All ventral arborizations, the commissures and innervations of further structures in the protocerebrum and the optic lobe developed in the pupal stages. However, most importantly, already in the first pupal stage, the main fiber tracts of the PDF neurons are present and structured like in the adult brain, with the difference that their number was smaller and the fiber tracts are not yet as thick (Figure 5–6). Similarly, all neuropils and central structures in the brain such as antennal lobes, mushroom bodies and central complex resembled already the adult structures (Figure 5a,d). In the optic lobes, the lamina had formed and was now HRP positive (Figure 5d). Lamina and medulla were separated by the first optic chiasma, and medulla and lobula by the second optic chiasma (Figure 5d). The serpentine layer between the proximal and distal part of the medulla had formed and the PDF fibers had extended along its entire dorso-ventral axis. However, they lost their prominence and the small dense PDF knot in the dorsal third of the serpentine layer had completely disappeared (Figure 5d,f,g). A few fibers appeared to leave the serpentine layer at its dorsal rim, a region that contains the medulla dorsal rim area (MEDRA), and ran dorso-laterally invading the dorsal rim area of the lamina (Figure 5f,g; Figure 6b,c; Figure 7e). Very similar to the PDF fibers in the knot of the larval medulla serpentine layer, the PDF fibers in the AME-like structure lost their density, and their staining intensity became weaker in pupae brains in relation to the fibers running to the central brain (Figure 5a,b). This is especially true in relation to the dense fibers in front of the lobula that innervate the anterior surface of the protocerebrum and give rise to the LVT that runs posteriorly and from which many PDF fibers split off (Figure 5c,e; Figure 6d; Figure 7d) (compare also with Beer et al., 2018). The only PDF fibers in the optic lobe that steadily increased their staining intensity throughout metamorphosis were those that invade the lamina dorsal rim area after passing the MEDRA (Figure 7e). Our detailed network complexity analysis showed a significant increase between the MEDRA and the dorsal lamina in P9 pupae brains (lateral POC: 10.6 ± 0.3, MEDRA: 4.5 ± 0.6) compared to P1 pupae brains (lateral POC: 6.6 ± 0.2, MEDRA: 0.8 ± 0.3). Otherwise, the PDF staining in the optic lobes remained rather weak until the end of pupal development.

In contrast to the optic lobes, the PDF fiber network in the central brain steadily grew and became denser and more complex during metamorphosis (Figures 6 and 7). Our detailed network complexity analysis showed a significant increase in protocerebral PDF fibers between bees of pupal stages P1 and P9. We analyzed differences in numbers of fibers in the anterior fiber plexus (AFP) passing by the vertical lobe (VL) of the mushroom body (Figure 7b) ($W = 7$, p-value $< .001$), the fibers building the ventral branch of the anterior optic commissure (vAOC) (Figure 7c) ($W = 9$, p-value $< .001$), the fibers running through the lateral posterior optic commissure (POC) close to the LVT (Figure 7d) ($W = 0$, p-value $< .001$) and the fibers leaving the MEDRA (Figure 7e) ($W = 4$, p-value $< .001$). There are approximately six PDF fibers running dorso-ventrally in the AFP close to the VL in P1 pupae

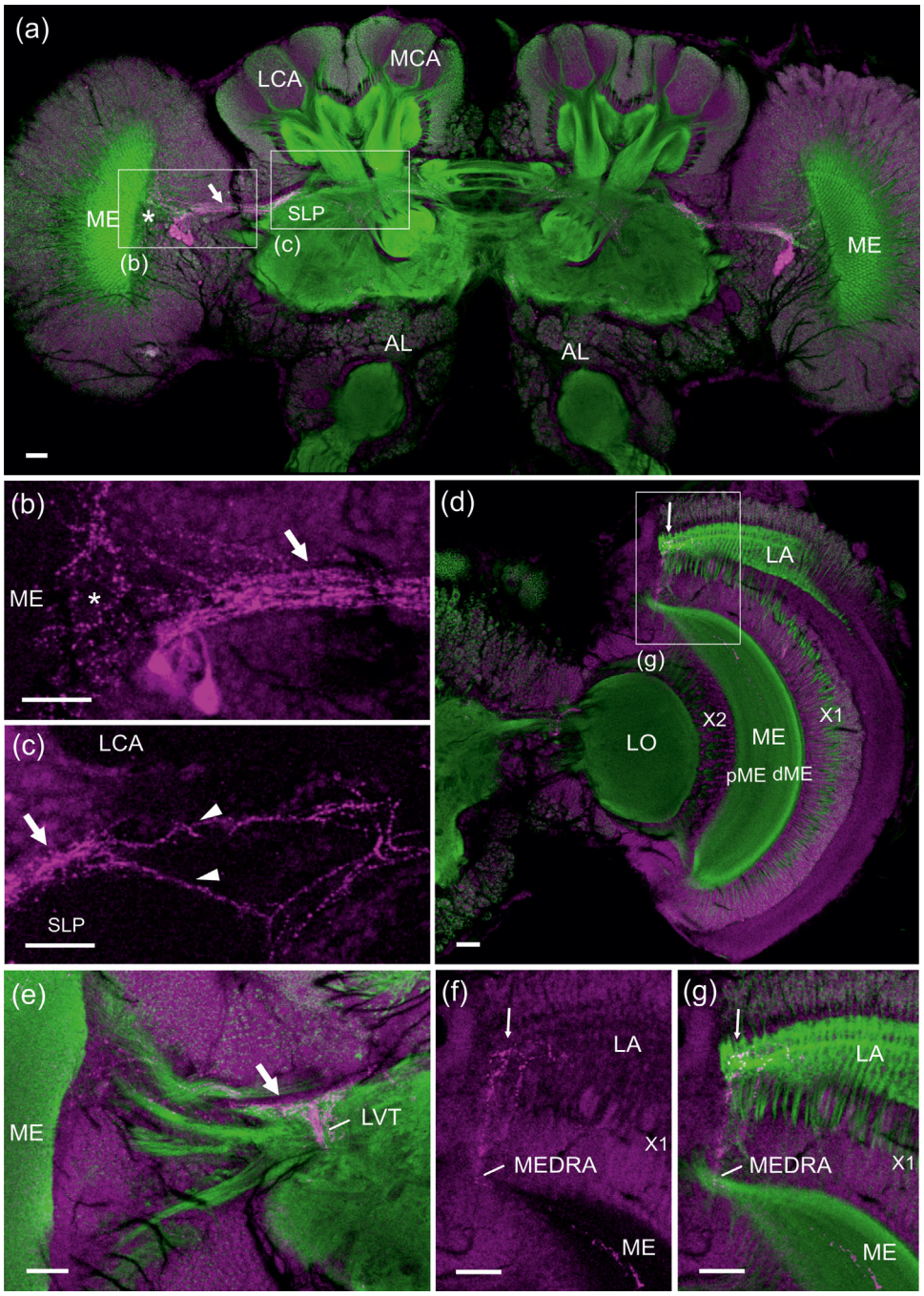

FIGURE 5 Pigment-dispersing factor (PDF) fibers in the brain of pupal stage 1. All images are projections of 10 confocal images (*z*-stack distance: 2 μm; pixel size: 1.07 μm) of vibratome sections, stemming from different areas and planes in the brain. Labeling is the same as in Figure 1. (a) Frontal overview of the brain without subesophageal ganglion from an anterior plane. The most prominent PDF labeling is present in the fiber tract (thick arrows) that connects the optic lobe and the accessory medulla (AME)-like structure (asterisk) with the superior lateral protocerebrum (SLP). This tract contains varicose PDF fibers and runs anteriorly of the lobula. It represents the beginning of the lobula valley tract (LVT). In a slightly more posterior plane (e), the LVT runs along the surface of the lobula, makes a loop and turns to the superior lateral protocerebrum. (b and c) Magnifications of the areas marked in (a), but without antihorseradish peroxidase (HRP) labeling; (b) shows that the AME-like structure (asterisk) contains fewer PDF varicosities than the fiber tract running toward the central brain (thick arrow); (c) shows the SLP in which the PDF fibers bifurcate into a more dorsal tract that runs ventrally of the lateral and medial mushroom body calyces (LCA and MCA) toward the dorsal midline of the brain and a more ventral tract that invades the medial part of the brain (arrow heads). (d) Right optic lobe from a posterior view. Lamina (LA), medulla (ME) and lobula (LO) are now strongly marked by HRP (green) and separated by the first (X1) and second (X2) optic chiasma. The PDF fibers have thin arborizations in the serpentine layer of the medulla that separates the proximal (pME) and distal (dME) parts of the medulla (ME). At the medulla dorsal rim area (MEDRA), some PDF fibers of the median layer fiber system appear to leave the serpentine layer (respectively medulla layer four in Madeira cockroach Arnold et al., 2020) and to run toward the dorsal rim of the lamina (thin arrow) connecting to the PDF arborization network of the posterior lamina. (f and g) Magnification of the area marked in (d). Scale bar: 50 µm

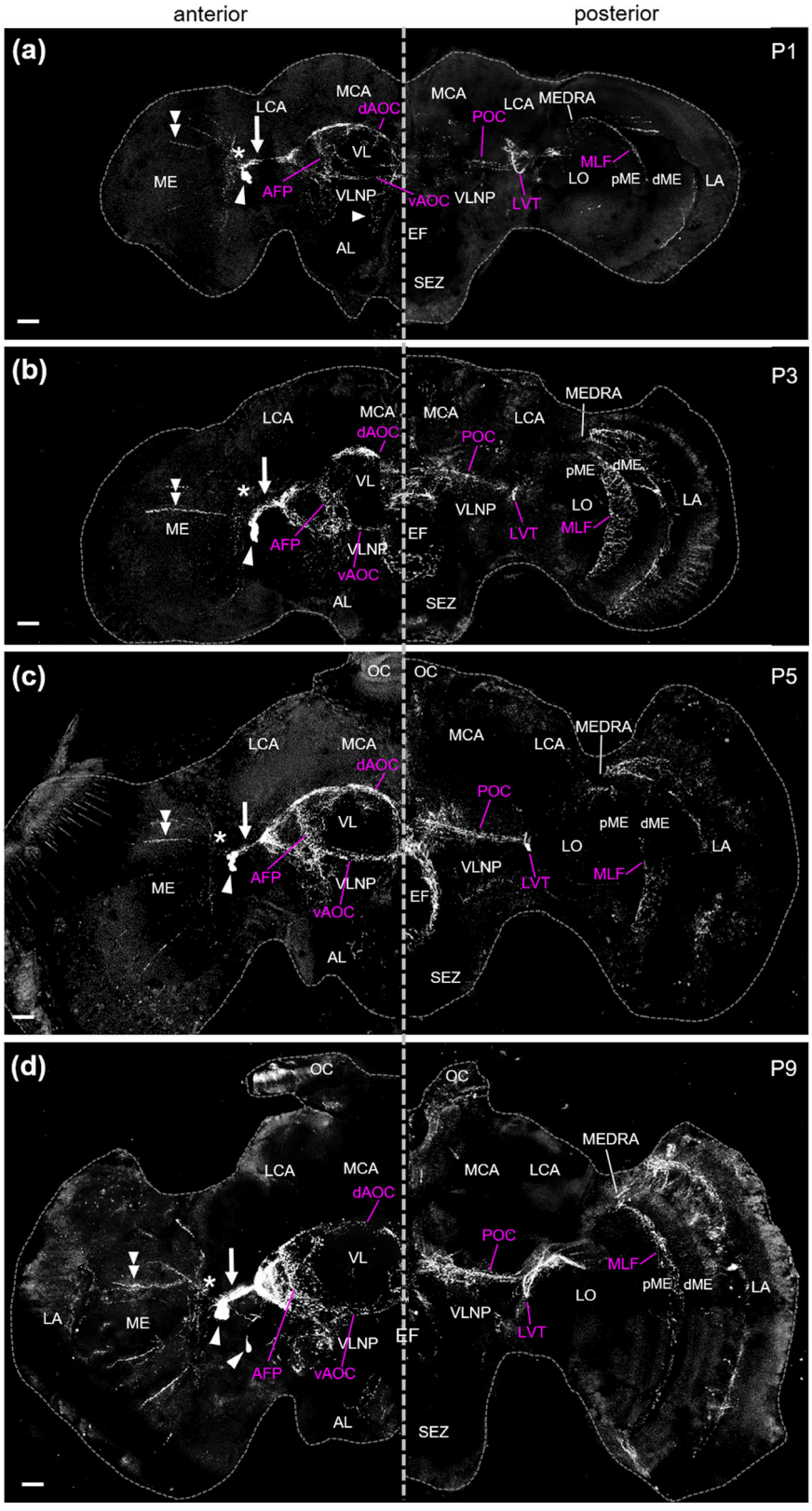

FIGURE 6 Overview of the increase in pigment-dispersing factor (PDF) neuronal network complexity throughout pupal development in honey bees. All images display overlays of 25–30 confocal sections (*z*-stack distance: 4 μm; pixel size: 1.07 μm) of whole mount brains. The anterior halves are shown to the left and the posterior halves are to the right. All are from a frontal view and the relevant pupal stage is indicated in the right upper corner, respectively. Note that these images are not meant to show details but just the general increase of thickness and labeling intensity of the PDF fibers that are all in principle already present in the first pupal stage (P1; compare also with Figure 3). For comparison with the PDF fibers in the adult brain please see Figure 7a). Cell bodies are marked by arrow heads, the accessory medulla (AME)-like structure by asterisks and the dense fiber hub, which significantly increased in thickness and staining intensity from (a) to (d) is marked by a thick arrow. Double arrow heads mark fibers in the anterior fiber fan that connects the AME-like structure with the PDF fiber network in the posterior lamina (LA). Abbreviations: AFP, anterior fiber plexus; AL, antennal lobe; EF, esophageal foramen; LA, lamina; LVT, lobula valley tract; (p/d)ME, (proximal/distal layer of the) medulla; LO, lobula; LCA and MCA, lateral and medial calyx of the mushroom body; MLF, median layer fiber system; OC, ocelli; POC, posterior optic commissure; VL, vertical lobe of the mushroom body; VLNP, ventrolateral neuropils of the protocerebrum; SEZ, subesophageal zone; v/dAOC, ventral/dorsal branch of the anterior optic commissure. Fiber tracts are labeled in magenta. Scale bar: 100 µm

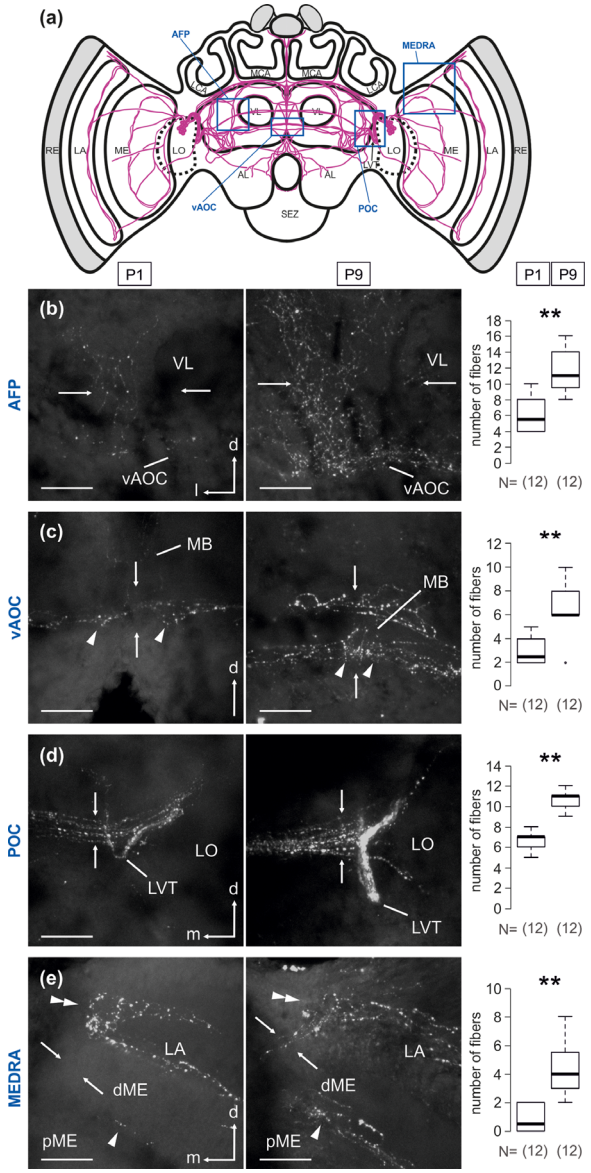

FIGURE 7 Complexity of clock network increases during honey bee development. (a) scheme of pigment-dispersing factor (PDF) neuron projections (in magenta) in the brain of the honey bee (adjusted from Beer et al., 2018). Areas of interest for analysis of fiber bundle complexity in (b–e) are marked with rectangles (blue). Images in (b–e) display frontal projections of confocal scans of brain areas (stacked confocal images in (b) 11 (P1) and 14 (P9); (c) 17 and 22; (d) 27 and 27; (e) 35 and 22; *z*-stack distance: 2.5 μm, pixel size: 0.22 μm), used to quantify PDF neuron fiber number in pupal stages P1 and P9. (b) Anterior fiber plexus (AFP) passing by the vertical lobe (VL) of the mushroom body; (c) fibers building the ventral branch of the anterior optic commissure (vAOC) (note that there is only one vAOC in P1, but in P9 a double commissure is build). (d) Fibers running through the lateral posterior optic commissure (POC) close to the densely innervated lobula valley tract (LVT), and (e) the fibers close to the dorsal rim area of the medulla (MEDRA). Arrows mark the plane in which we quantified fibers crossing this plane perpendicular. In P1, only few fibers run in close proximity to the MEDRA and very few PDF fibers run between the proximal (pME) and distal layer (dME) of the medulla (arrow head), while the dorsal rim area of the lamina (double arrow head) shows several fibers. Arrow heads in (b) point to fibers that were not quantified because they project not contralaterally, but into the median bundle (MB). Abbreviations: AL, antennal lobe; LA, lamina; LO, lobula; LCA/MCA, lateral/medial calyx of the mushroom bodies; RE, retina; SEZ, subesophageal zone; VL, vertical lobe of the mushroom bodies. Scale bar: 50 μm. Differences in number of fibers in the specific areas are displayed in boxplots; sample sizes are indicated in grey with the sample group

(6.2 ± 0.6, mean ± STE), while in P9 pupae, there is double the amount (12.1 ± 1.1, mean ± STE) and the fibers start to wrap the VL closely (Figure 7b). PDF fibers in the vAOC of P1 pupae are very few (3.0 ± 0.4, mean ± STE) and build one commissure bundle, while in P9 the fibers (6.7 ± 0.6, mean ± STE) build a double commissure (Figure 7c). Along the fibers of the vAOC in P9, there are several fibers running dorsally into the median bundle (MB), but not contralaterally (Figure 7c, arrow heads). These fibers were excluded from the quantification because their projection pattern is different from the neuron fibers we quantified in P1 brains in the vAOC. Similarly, we found more PDF fibers in the lateral POC (Figure 7d).

4.3 | Detailed analysis of soma size and staining intensity of the PDF neurons

In contrast to fruit flies and cockroaches, the PDF neurons could not be classified into different cell types by measuring somata sizes. However, plotting the distribution of cell body sizes in the different developmental stages showed a highly different pattern for cell body sizes in L3 compared to all other stages (Figure 8). There is a narrow peak around the size of 17.5 μm^2 for PDF cells in L3, while all other stages display a broad distribution of differently sized cell bodies. The peaks of earlier pupal stages indicate prevailing cell sizes of around 25.6–27.3 μm^2 and peak cell sizes become bigger with developmental stages. Most abundant cell body size of PDF cells is 40.4 μm^2 in the last pupal stage P9. In P3 and P5, a second peak is detectable. The broad distribution and occasionally two peaks of prevalent PDF cell body sizes in the stages L5 to P9 may indicate different subpopulations of the PDF neuron cluster in honey bees. Therefore, we investigated whether PDF production (indicated by staining intensity) and location of PDF cell bodies in the brain correlates with the different sizes. We found that cell body size positively correlates with staining intensity in pupae and larval instar five brains (Figure 8a/c) (see Table 2 for results of Kendall's rank correlation test) as well as relative position in the brains of pupae (Figure 9b). In pupae, larger PDF somata were located more anteriorly in the brain than smaller PDF somata. We could not detect such a correlation of larger cell bodies located more anteriorly in the brain of larvae (Figure 9d/f). There was also no correlation of cell body size and staining intensity of PDF neurons of L3 larvae (Figure 9e).

5 | DISCUSSION

In fruit flies and cockroaches, it has been demonstrated that specific PDF neurons are substantial to the basic clock network structure also involved in regulation of the circadian clock output behavior (Arnold

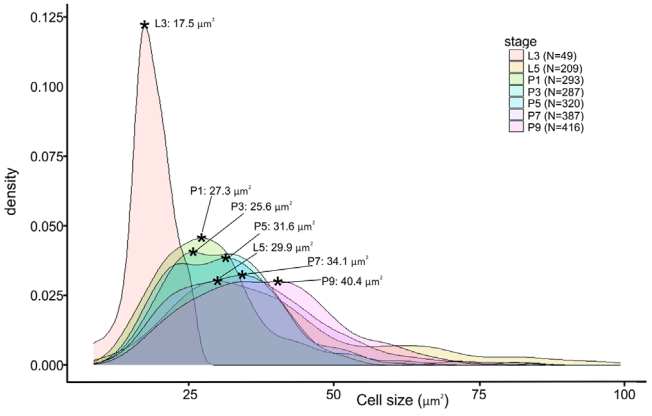

FIGURE 8 Cell body size of pigment-dispersing factor (PDF) neurons during different stages of development. Density plot for the cell body sizes of PDF neurons of bees in different developmental stages. Peaks of the density curve are marked with an asterisk for each group. Sample sizes are indicated with the sample group

TABLE 2 Statistical data of Kendall's correlation tests investigating correlation of cell body size with staining intensity and relative position in the brain of pupae and the two larval instars L3 and L5

Correlation of cell body size with staining intensity:			
	Test statistic	*p*-Value	τ
Pupae	12.57	< .01	0.20
L5 larvae	3.79	< .01	0.18
L3 larvae	576	.8437	−0.02
Correlation of cell body size with relative position in the brain:			
	Test statistic	*p*-Value	τ
Pupae	15.84	< .01	0.27
L5 larvae	0.50	.62	0.02
L3 larvae	−0.65	.51	−0.07

et al., 2020; Gestrich et al., 2018; Giese et al., 2018; Klose et al., 2016; Schlichting et al., 2016). A similar role of a subset of the PDF neurons is likely in the honey bee, but in adults it was so far not possible to classify individual PDF neurons (Beer et al., 2018), as it has been done in flies and cockroaches (Helfrich-Förster et al., 2007; Reischig & Stengl, 2003b). Here, we tried to identify possible differences in neuroanatomy and associated function of different PDF neurons by describing the development of the PDF network.

5.1 | The first three PDF neurons in the third larval instar of the bee resemble to some degree the small ventrolateral neurons of *Drosophila* and the first PDF neurons in locust embryos

The neurites of the first three PDF neurons that are visible in the third larval instar of the bee form a varicose network at the base of the developing medulla and run into the superior lateral protocerebrum, where they terminate ventrally of the calyces of the developing mushroom bodies. Their shape strongly resembles those in locust embryos (Homberg & Prakash, 1996) and fly larvae (Helfrich-Förster, 1997): locusts and flies possess four PDF neurons at 50% of embryonic and larval development, respectively, which also project into the superior lateral protocerebrum. In flies, these neurons are the small ventrolateral PDF neurons, the terminals of which terminate anteriorly and ventrally of the calyces of the mushroom bodies in larvae, pupae and adults (Helfrich-Förster, 1997). Like in bees, the larval *Drosophila* PDF somata have a round shape and they are initially rather small. During larval development, they continuously grow and, at the beginning of metamorphosis, they reach the same size as the newly born four large PDF neurons that appear at about 50% of metamorphosis. The latter then strongly grow, and at the time of eclosion, they are three times larger than the small PDF neurons (Helfrich-Förster, 1997). Also in locust embryos, the size of the first appearing PDF neurons appears small (Homberg & Prakash, 1996), and similarly, adult cockroaches possess four PDF neurons with small and round somata in the group of PDF cell located anterior of the medulla (aPDFMEs) (Reischig & Stengl, 2003b); reviewed in Stengl & Arendt, 2016). This suggests that the three first PDF neurons of honey bees are homologous to small PDF neurons of these hemimetabolous insects. The four small cockroach PDF neurons are local neurons that terminate in the ipsilateral AME. Similarly, the three bee PDF neurons send predominantly fibers into the AME-like structure. Nevertheless, we did also see faint projections in the superior lateral protocerebrum, which is reminiscent of the PDF fibers seen in fruit fly larvae and locust embryos. It is difficult to judge whether these fibers stem from all or just one of the small PDF neurons or perhaps even from a fourth PDF neuron with larger soma that has just appeared (sometimes we found four PDF neurons in third larval instars). What we can say is that the appearance of additional PDF neurons with larger somata in fifth instar larvae is accompanied with the appearance of fibers that run into the medial protocerebrum and into the lateral medulla (see below). Therefore, it is very likely that the first three PDF neurons in bee larvae correspond to the first four PDF neurons of flies and locusts and that these represent a subcluster of the PDF neurons, which project solely to the AME and perhaps additionally to the superior lateral protocerebrum. In any case, their projections are limited to the ipsilateral brain hemisphere. As found in flies and cockroaches, this PDF sub cluster may have a special function in the circadian system of bees (Gestrich et al., 2018; Helfrich-Förster et al., 2007; Klose et al., 2016; Reischig & Stengl, 2003b; Wei et al., 2014), but this has to be determined in future studies.

5.2 | The following PDF neurons have larger somata and project toward the distal optic lobe and invade medial areas of the protocerebrum

Although our results—including the density curves of the cell body sizes–indicate that there is only one population of PDF cells in the third larval instar (narrow distribution of the cell sizes), there may exist

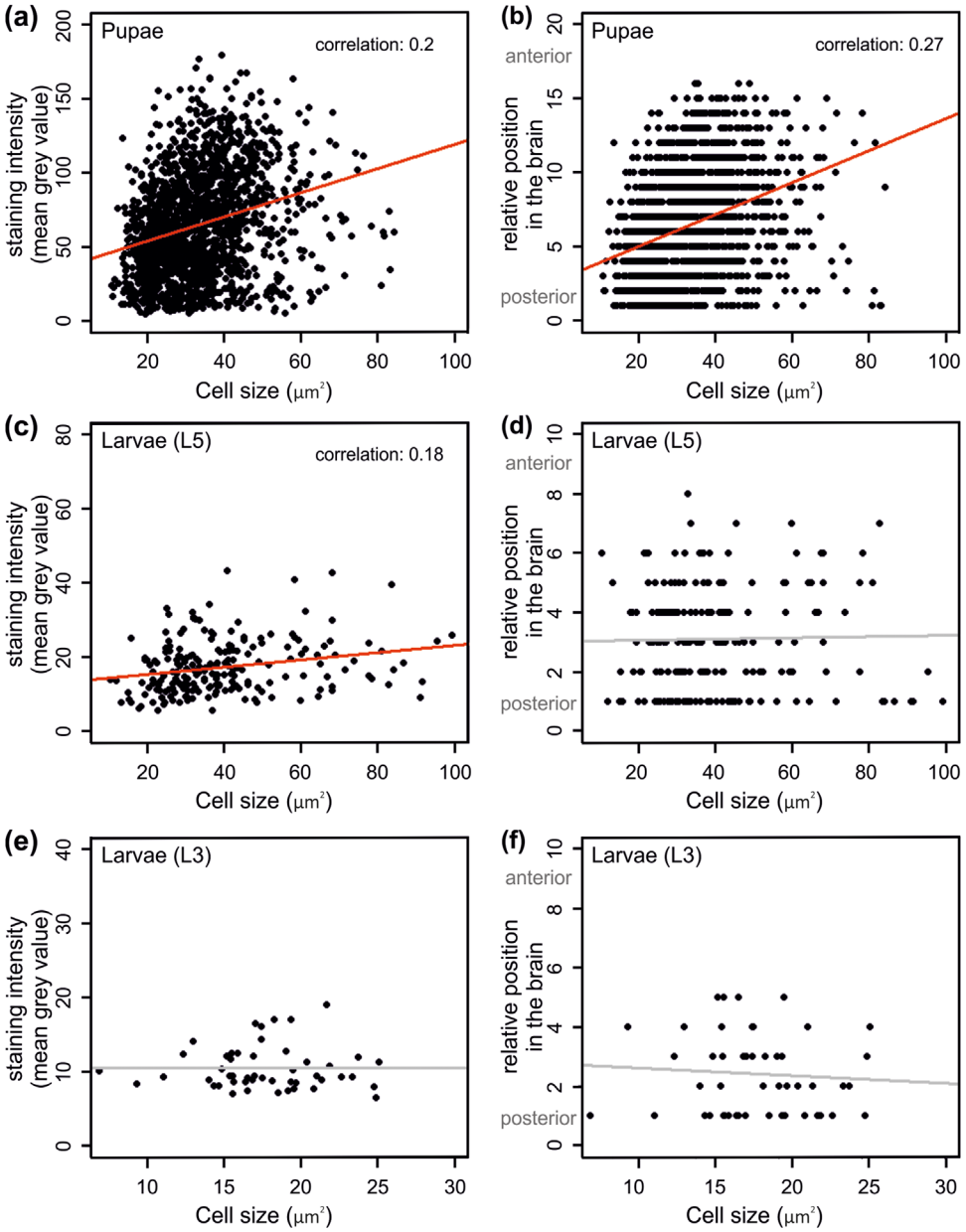

FIGURE 9 Correlation analysis of pigment-dispersing factor (PDF) cell body sizes with staining intensity and relative position in the brains. In pupae, cell size of PDF neurons correlates positively with staining intensity (a) and relative anterior position in the brain (b). In L5 larvae, this is only true for staining intensity (c), but there is no significant correlation of PDF cell body size and relative position in the brain (d). There is no correlation of staining intensity (e) or relative position (f) with cell sizes in L3 larvae brains. Significant correlation ratio is indicated in the plot (Kendall's rank correlation tau) and by a red regression line. A grey regression line indicates no significant correlation

several populations from the fifth larval instar onward. We found a broad distribution of cell sizes, and in some cases even two maxima. This clearly points to two or even more subpopulations of PDF cells defined by soma size. In the cockroach, the larger aPDFME neurons could be classified into one largest, three large and four medium sized neurons (Giese et al., 2018; Reischig & Stengl, 2003b; Wei et al., 2014), but such a classification was not possible in the honey bee. We rather found a gradual distribution in the size of PDF cell bodies in all developmental stages after L3 although we could sometimes see a very large neuron in an anterior position of the brain and large neurons generally had the tendency to be farther from the AME-like structure than the small ones: we found a positive correlation between cell body size and anterior position in the brain in pupal brains (the more anterior, the larger the distance to the AME-like structure). As already mentioned, the first neurons with large soma size appeared in the fifth larval instar, and this resulted in a clear shift to larger cell sizes in the density curve from L3 to L5. The shift between L3 and L5 was especially large, probably because the three small cell bodies had also grown in the meantime (see above). A second shift to larger cell body sizes occurred during pupal development between P7 and P9. Furthermore, from L5 onward,

we found a significant correlation of cell body size with mean staining intensity, which may indicate that smaller and larger PDF neurons produce different amounts of PDF. In cockroaches, the size and staining intensity of the PDF neurons correlate with the width of their arborizations, meaning that the projections of the largest and most intensively stained cells reach very far (e.g., to the contralateral optic lobe) (Wei et al., 2010). In addition, the cell bodies of the large PDF neurons are located more distantly of the AME than the cell bodies of the smaller ones as we found in the honey bee.

We were not able to distinguish the projections of medium sized and large PDF neurons in honey bees, but we noticed that the projections extended into the distal optic lobe and into the medial protocerebrum as soon as the larger neurons appeared. This process continued during metamorphosis, but notably contralateral projections and main connections to the different brain areas seem already largely established in bee pupal stage 1, while in *Drosophila* contralateral projections are formed only in later pupal stages (Helfrich-Förster, 1997). The new PDF neurons most likely build connections to PDF-negative clock neurons in the central brain as well as to different neurons downstream the clock (Beer et al., 2018). For example, the connections to the dorsal brain of the larvae may be important for the integration of time information into olfactory learning processed in the calyces of the mushroom bodies (Gronenberg & Lopez-Riquelme, 2004). Whether this is of biological relevance to the larva inside the hive surrounded by food and not submitted to environmental changes is debatable. The later developing arborizations in the central brain (especially the central complex) may integrate the clock into downstream behavior like locomotor activity and sleep (Pfeiffer & Homberg, 2014; Strauss & Heisenberg, 1993), as happens for the cockroach clock (Gestrich et al., 2018). Furthermore, the contralateral projections may constitute direct coupling pathways between the two pacemaker centers in both lateral hemispheres, as has been demonstrated in cockroaches, and the extra-large PDF neuron may be especially important because it projects via the posterior optic commissure to the posterior optic tubercles that are closely associated with the central complex that mediates spatial orientation and locomotor activity programs (Pan et al., 2009; Pfeiffer & Homberg, 2014; Reischig et al., 2004; Reischig & Stengl, 2002; Strauss & Heisenberg, 1993).

5.3 | The optic lobe projections of the PDF neurons are less dense and less elaborate compared to those of hemimetabolous insects

In comparison to the PDF arborizations in the central brain, the projections to the optic lobes are clearly less dense and especially those in the lamina develop later than in locusts and putatively also cockroaches. There are two plausible reasons for this difference: (1) the honey bee does not possess posterior PDF neurons and (2) the honey bee lacks the two groups of PDF-positive lamina neurons that project into lamina and medulla and that intermingle with the fibers deriving from the aPDFMes in cockroaches (Arnold et al., 2020; Gestrich et al., 2018). Thus, the 15 PDF neurons described are the only cells that contribute to the PDF arborizations in the optic lobe of the bee. The relatively weak innervation of the optic lobes by PDF fibers may point to a lower importance of light input pathways to the clock in comparison to other insects (see below). Among all PDF fibers in the optic lobe, the ones in the dorsal rim area of the lamina are the most prominent ones at the end of metamorphosis. This may be of later functional relevance since this region is involved in honey bee sky compass orientation (Zeller et al., 2015).

5.4 | Honey bee larvae appear to possess an AME-like structure, but the density of PDF fibers in this structure diminishes during metamorphosis

As already mentioned above, the larval PDF network at the base of the medulla is very similar in structure and position to the AME of hemimetabolous insects (Homberg et al., 1991; Homberg & Prakash, 1996; Stengl & Homberg, 1994), and for this reason we called it an AME-like structure. Like the locust and cockroach AME, the bee AME-like structure was rich of varicose PDF fibers that arborized in a non-retinotopic manner. Although the AME of locusts and cockroaches has an ovoid shape, just judged from the PDF immunostaining, the AME-like structure of honey bees was rather flat. It became even flatter during larval development when it extended in the direction of the distal medulla. In flies, the AME has also no ovoid shape, it is flatter than in cockroaches and fused with the medulla. However, the AME of flies does not show prominent varicose PDF fibers as does the AME-like structure of honey bees. The fly AME stems from the larval optic neuropil, which is innervated by the larval eyes (stemmata) as is true for other holometabolous insects (Fleissner & Fleissner, 2003; Hagberg, 1986; Hanström, 1940; Helfrich-Förster et al., 2002). Therefore, the larval optic neuropil contains mostly fine dendritic fibers from neurons that are postsynaptic to the photoreceptor cells. Indeed, fine dendritic PDF fibers from the four small PDF neurons invade the larval optic neuropil and later the AME in *Drosophila*. They get direct inputs from photoreceptor cells, of Bolwig's organ in larvae and early pupae, and of the Hofbauer–Buchner eyelets in late pupae and adults (Helfrich-Förster et al., 2002; Yasuyama & Meinertzhagen, 1999). The cockroach AME does not get direct photoreceptor inputs, but it receives light information via the PDF neurons in the lamina that are connected to eyes and lamina organs and project into the AME (Arnold et al., 2020). Thus, the circadian clock center in the AME of cockroaches is "well connected" with the photic environment, which appears necessary since cockroach nymphs are freely moving and their clock needs to be synchronized with the external light-dark cycle.

5.5 | Photic input to circadian clock in honey bees may be less crucial than for other insects

Honey bees remain in the dark hive during their entire development and still as adult nurse bees. Thus, vision and light input to the circadian clock is not important for them until they leave the hive as forager

bees. Consequently, their circadian system develops slowly and is not yet mature when they eclose from their pupa (Beer et al., 2016; Beer & Helfrich-Förster, 2020b; Eban-Rothschild et al., 2012; Fuchikawa et al., 2016). The same is true for their visual system. They lack larval stemmata (Gilbert, 1994), and their compound eyes mature late with the photoreceptor cells achieving their final opsin composition only before they leave the hive as forager bees (Lichtenstein et al., 2018). Perhaps, as a result, social cues and not the light-dark cycle serve as major zeitgeber for the circadian clock of honey bees (Beer et al., 2016; Fuchikawa et al., 2016). Environmental signals that could synchronize the clock of honey bees and therefore serve as social cues were suggested to be of either thermal, hygroscopic, chemical (pheromones) or vibrational nature or a combination, but no direct physical contact is needed (Beer et al., 2016; Fuchikawa et al., 2016; Moritz & Kryger, 1994; Siehler & Bloch, 2020). If temperature signals are of significant importance for social synchronization of honey bees residing in the thermoregulated hive is debatable because the minimum amplitude in temperature changes that can entrain the honey bee clock is approximately 6–10°C (Fuchikawa & Shimizu, 2007; Moore & Rankin, 1993). Individual bees cannot create a microenvironment with this high temperature amplitudes, but they synchronize to each other in air connected compartments or residing on the same substrate (Siehler et al., 2021). Therefore, vibrational signals and volatiles seem to play an important role for synchronizing rhythms in the bee hive. After the compound eye is completely developed, light may become more important as a zeitgeber than before. However, when we compare the phase response curves in activity shifts induced by 1 h light pulses applied to cockroaches, flies and honey bees, we find that the honey bees shift their activity maximal by only 1.5–2 h, but cockroaches and flies shift their activity up to 4–5 h/day (Fuchikawa & Shimizu, 2008; Ludin et al., 2012; Saunders et al., 1994; Saunders & Thomson, 1977). This points also to a less light sensitive system in the honey bee. Very similar, the developing circadian clock of solitary bees does rely less on photic input. The daily emergence of solitary bees is synchronized rather by temperature cycles than daily light-dark cycles (Beer et al., 2019; Bennett et al., 2018; Tweedy & Stephen, 1970). Light sensitivity of the circadian clock seems to increase only after the solitary bees have eclosed from their pupal case and wait to emerge from their cocoon. From that time onward, their activity can immediately synchronize to light-dark cycles of low light intensity (Beer et al., 2019).

Altogether the different life style of honey bees in comparison to flies and cockroaches can explain why the AME does not play a major role in their circadian system and why the AME does not further develop after its initial birth in the third larval instar. It is possible that the missing input from larval photoreceptor cells is the reason why the PDF network in the AME-like structure gets sparse at the beginning of metamorphosis and finally a new PDF fiber hub in front of the lobula develops. Nevertheless, we cannot exclude that the AME-like structure of honey bees is involved in nonphotic input pathways to the circadian clock, which was suggested in cockroaches (Schulze et al., 2013). It will be highly interesting to test which environmental cues are effective to entrain the clock of developing honey bees and whether the AME-like structure is involved in the pathway that synchronizes the circadian clock to environmental cycles.

In summary, our study reveals interesting differences in the development of the PDF network between honey bees, flies and cockroaches which may have their basis in the different life styles of these three insects. In all three insects, the PDF-positive clock neurons are important components of the circadian system and they appear composed of different neuronal subclusters fulfilling specific functions in circadian system. In honey bees, the circadian clock neuronal network systematically grows and gets more complex throughout development. This made the characterization of different PDF subclusters difficult. Nevertheless, future studies on clock development in honey bees appear promising since they may help to understand the highly complex rhythmic behavior of honey bees.

ACKNOWLEDGMENTS

This research was funded by the German Research Foundation CRC 1047 "Insect Timing" (project A1 and C2). Katharina Beer was furthermore supported by a grant of the German Excellence Initiative to the Graduate School of Life Sciences, University of Würzburg and the SCIENTIA career development program of the University of Würzburg. Further acknowledgements go to Beate Krischke for technical assistance in the laboratory. We also want to thank Heinrich Dircksen for providing the PDH antibody, Ingolf Steffan-Dewenter for providing work space in the laboratory and Thomas Raabe and Keram Pfeiffer for discussions.

Open access funding enabled and organized by Projekt DEAL.

CONFLICT OF INTEREST

The authors declare no conflict of interest.

AUTHOR CONTRIBUTIONS

Katharina Beer collected and analyzed the data. Katharina Beer and Charlotte Helfrich-Förster compiled figures and wrote the manuscript. Charlotte Helfrich-Förster conceived the project. Charlotte Helfrich-Förster and Stephan Härtel contributed to funding and revised the manuscript.

DATA AVAILABILITY STATEMENT

The data that support the findings of this study are available from the corresponding author upon reasonable request.

PEER REVIEW

The peer review history for this article is available at https://publons.com/publon/10.1002/cne.25278.

ORCID

Katharina Beer https://orcid.org/0000-0001-5436-6735
Charlotte Helfrich-Förster https://orcid.org/0000-0002-0859-9092

REFERENCES

Arnold, T., Korek, S., Massah, A., Eschstruth, D., & Stengl, M. (2020). Candidates for photic entrainment pathways to the circadian clock via optic lobe neuropils in the Madeira cockroach. *Journal of Comparative Neurology*, *528*(10), 1754–1774. https://doi.org/10.1002/cne.24844

Aupinel, P., Fortini, D., Dufour, H., Tasei, J., Michaud, B., Odoux, J., & Pham-Delegue, M. (2005). Improvement of artificial feeding in a standard *in vitro* method for rearing *Apis mellifera* larvae. *Bulletin of Insectology*, *58*(2), 107.

Aupinel, P., Fortini, D., Michaud, B., Marolleau, F., Tasei, J.-N., & Odoux, J.-F. (2007). Toxicity of dimethoate and fenoxycarb to honey bee brood (*Apis mellifera*), using a new *in vitro* standardized feeding method. *Pest Management Science*, *63*(11), 1090–1094. https://doi.org/10.1002/ps.1446

Beer, K., & Helfrich-Förster, C. (2020). Model and Non-model Insects in Chronobiology. *Frontiers in Behavioral Neuroscience*, *14*, https://doi.org/10.3389/fnbeh.2020.601676

Beer, K., & Helfrich-Förster, C. (2020b). Post-embryonic development of the circadian clock seems to correlate with social life style in bees. *Frontiers in Cell and Developmental Biology*, *8*, 581323. https://doi.org/10.3389/fcell.2020.581323

Beer, K., Kolbe, E., Kahana, N. B., Yayon, N., Weiss, R., Menegazzi, P., Bloch, G., & Helfrich-Förster, C. (2018). Pigment-Dispersing Factor-expressing neurons convey circadian information in the honey bee brain. *Open Biology*, *8*(1), 170224. https://doi.org/10.1098/rsob.170224

Beer, K., Schenk, M., Helfrich-Förster, C., & Holzschuh, A. (2019). The circadian clock uses different environmental time cues to synchronize emergence and locomotion of the solitary bee *Osmia bicornis*. *Scientific Reports*, *9*(1), 17748. https://doi.org/10.1038/s41598-019-54111-3

Beer, K., Steffan-Dewenter, I., Härtel, S., & Helfrich-Förster, C. (2016). A new device for monitoring individual activity rhythms of honey bees reveals critical effects of the social environment on behavior. *Journal of Comparative Physiology A*, *202*(8), 555–565. https://doi.org/10.1007/s00359-016-1103-2

Beling, I. (1929). Über das Zeitgedächtnis der Bienen. *Zeitschrift Für Vergleichende Physiologie*, *9*(2), 259–338. https://doi.org/10.1007/BF00340159

Bennett, M. M., Rinehart, J. P., Yocum, G. D., Doetkott, C., & Greenlee, K. J. (2018). Cues for cavity nesters: Investigating relevant zeitgebers for emerging leafcutting bees, *Megachile rotundata*. *The Journal of Experimental Biology*, *221*(10), jeb175406. https://doi.org/10.1242/jeb.175406

Bloch, G., Bar-Shai, N., Cytter, Y., & Green, R. (2017). Time is honey: Circadian clocks of bees and flowers and how their interactions may influence ecological communities. *Philosophical Transactions of the Royal Society B: Biological Sciences*, *372*(1734), 20160256. https://doi.org/10.1098/rstb.2016.0256

Bloch, G., Solomon, S. M., Robinson, G. E., & Fahrbach, S. E. (2003). Patterns of PERIOD and pigment-dispersing hormone immunoreactivity in the brain of the European honeybee (*Apis mellifera*): Age- and time-related plasticity. *The Journal of Comparative Neurology*, *464*(3), 269–284. https://doi.org/10.1002/cne.10778

Cheeseman, J. F., Winnebeck, E. C., Millar, C. D., Kirkland, L. S., Sleigh, J., Goodwin, M., Pawley, M. D. M., Bloch, G., Lehmann, K., Menzel, R., & Warman, G. R. (2012). General anesthesia alters time perception by phase shifting the circadian clock. *Proceedings of the National Academy of Sciences*, *109*(18), 7061–7066. https://doi.org/10.1073/pnas.1201734109

Dircksen, H., Zahnow, C. A., Gaus, G., Keller, R., Rao, K. R., & Riehm, J. P. (1987). The ultrastructure of nerve endings containing pigment-dispersing hormone (PDH) in crustacean sinus glands: Identification by an antiserum against a synthetic PDH. *Cell and Tissue Research*, *250*(2), 377–387. https://doi.org/10.1007/BF00219082

Dunlap, J. C. (1999). Molecular bases for circadian clocks. *Cell*, *96*(2), 271–290. https://doi.org/10.1016/S0092-8674(00)80566-8

Eban-Rothschild, A., Shemesh, Y., & Bloch, G. (2012). The colony environment, but not direct contact with conspecifics, influences the development of circadian rhythms in honey bees. *Journal of Biological Rhythms*, *27*(3), 217–225. https://doi.org/10.1177/0748730412440851

Elekes, K., & Nässel, D. R. (1999). Pigment-dispersing hormone-like immunoreactive neurons in the central nervous system of the gastropods, *Helix pomatia* and *Lymnaea stagnalis*. *Cell and Tissue Research*, *295*(2), 339–348. https://doi.org/10.1007/s004410051240

Fleissner, G., & Fleissner, G. (2003). Nonvisual photoreceptors in arthropods with emphasis on their putative role as receptors of natural Zeitgeber stimuli. *Chronobiology International*, *20*(4), 25. https://doi.org/10.1081/CBI-120023679

Fleissner, G., Loesel, R., Fleissner, G., Waterkamp, M., Kleiner, O., Batschauer, A., & Homberg, U. (2001). Candidates for extraocular photoreceptors in the cockroach suggest homology to the lamina and lobula organs in beetles. *The Journal of Comparative Neurology*, *433*(3), 401–414. https://doi.org/10.1002/cne.1148

Fuchikawa, T., Beer, K., Linke-Winnebeck, C., Ben-David, R., Kotowoy, A., Tsang, V. W. K., Warman, G. R., Winnebeck, E. C., Helfrich-Förster, C., & Bloch, G. (2017). Neuronal circadian clock protein oscillations are similar in behaviourally rhythmic forager honeybees and in arrhythmic nurses. *Open Biology*, *7*(6), 170047. https://doi.org/10.1098/rsob.170047

Fuchikawa, T., Eban-Rothschild, A., Nagari, M., Shemesh, Y., & Bloch, G. (2016). Potent social synchronization can override photic entrainment of circadian rhythms. *Nature Communications*, *7*, 11662. https://doi.org/10.1038/ncomms11662

Fuchikawa, T., & Shimizu, I. (2007). Circadian rhythm of locomotor activity in the Japanese honeybee, *Apis cerana japonica*. *Physiological Entomology*, *32*(1), 73–80. https://doi.org/10.1111/j.1365-3032.2006.00543.x

Fuchikawa, T., & Shimizu, I. (2008). Parametric and nonparametric entrainment of circadian locomotor rhythm in the Japanese honeybee *Apis cerana japonica*. *Biological Rhythm Research*, *39*(1), 57–67. https://doi.org/10.1080/OO2glO10701318188

Gestrich, J., Giese, M., Shen, W., Zhang, Y., Voss, A., Popov, C., Stengl, M., & Wei, H. (2018). Sensitivity to pigment-dispersing factor (PDF) is cell-type specific among PDF-expressing circadian clock neurons in the Madeira cockroach. *Journal of Biological Rhythms*, *33*(1), 35–51. https://doi.org/10.1177/0748730417739471

Giese, M., Gestrich, J., Massah, A., Peterle, J., Wei, H., & Stengl, M. (2018). GABA- and serotonin-expressing neurons take part in inhibitory as well as excitatory input pathways to the circadian clock of the Madeira cockroach *Rhyparobia maderae*. *European Journal of Neuroscience*, *47*(9), 1067–1080. https://doi.org/10.1111/ejn.13863

Gilbert, C. (1994). Form and function of stemmata in larvae of holometabolous insects. *Annual Review of Entomology*, *39*(1), 323–349. https://doi.org/10.1146/annurev.en.39.010194.001543

Groh, C., & Rössler, W. (2008). Caste-specific postembryonic development of primary and secondary olfactory centers in the female honeybee brain. *Arthropod Structure & Development*, *37*(6), 459–468. https://doi.org/10.1016/j.asd.2008.04.001

Gronenberg, W., & Lopez-Riquelme, G. O. (2004). Multisensory convergence in the mushroom bodies of ants and bees. *Acta Biologica Hungarica*, *55*(1–4), 31–37. https://doi.org/10.1556/ABiol.55.2004.1-4.5

Hagberg, M. (1986). Ultrastructure and central projections of extraocular photoreceptors in caddiesflies (Insecta: Trichoptera). *Cell and Tissue Research*, *245*(3), 643–648. https://doi.org/10.1007/BF00218567

Hanström, B. (1940). *Inkretorische organe, Sinnesorgane und Nervensystem des Kopfes einiger niederer Insektenordnungen: Vol. Kungl Sven Vetensk Akad Handl Ser III* (18th ed.). Almquist & Wiksells.

Helfrich-Förster, C. (1997). Development of pigment-dispersing hormone-immunoreactive neurons in the nervous system of *Drosophila melanogaster*. *Journal of Comparative Neurology*, *380*(3), 335–354. https://doi.org/10.1002/(SICI)1096-9861(19970414)380:3%3c335::AID-CNE4%3e3.0.CO;2-3

Helfrich-Förster, C. (2005). *Organization of endogenous clocks in insects*. Portland Press Limited.

Helfrich-Förster, C. (2020). Light input pathways to the circadian clock of insects with an emphasis on the fruit fly *Drosophila melanogaster*. *Journal*

of Comparative Physiology A, *206*(2), 259–272. https://doi.org/10.1007/s00359-019-01379-5

Helfrich-Förster, C., Edwards, T., Yasuyama, K., Wisotzki, B., Schneuwly, S., Stanewsky, R., Meinertzhagen, I. A., & Hofbauer, A. (2002). The extraretinal eyelet of *Drosophila*: Development, ultrastructure, and putative circadian function. *Journal of Neuroscience*, *22*(21), 9255–9266. https://doi.org/10.1523/JNEUROSCI.22-21-09255.2002

Helfrich-Förster, C., Nitabach, M. N., & Holmes, T. C. (2011). Insect circadian clock outputs. *Essays in Biochemistry*, *49*, 87–101. https://doi.org/10.1042/bse0490087

Helfrich-Förster, C., Shafer, O. T., Wülbeck, C., Grieshaber, E., Rieger, D., & Taghert, P. (2007). Development and morphology of the clock-gene-expressing lateral neurons of *Drosophila melanogaster*. *The Journal of Comparative Neurology*, *500*(1), 47–70. https://doi.org/10.1002/cne.21146

Helfrich-Förster, C., Stengl, M., & Homberg, U. (1998). Organization of the circadian system in insects. *Chronobiology International*, *15*(6), 567–594. https://doi.org/10.3109/07420529808993195

Helfrich-Förster, C., Täuber, M., Park, J. H., Mühlig-Versen, M., Schneuwly, S., & Hofbauer, A. (2000). Ectopic expression of the neuropeptide pigment-dispersing factor alters behavioral rhythms in *Drosophila melanogaster*. *Journal of Neuroscience*, *20*(9), 3339–3353. https://doi.org/10.1523/JNEUROSCI.20-09-03339.2000

Hendriksma, H. P., Härtel, S., & Steffan-Dewenter, I. (2011). Honey bee risk assessment: New approaches for *in vitro* larvae rearing and data analyses. *Methods in Ecology and Evolution*, *2*(5), 509–517. https://doi.org/10.1111/j.2041-210X.2011.00099.x

Homberg, U., & Prakash, N. (1996). Development of pigment-dispersing hormone-like immunoreactivity in the brain of the locust *Schistocerca gregaria*: Comparison with immunostaining for urotensin I and Mas-allatotropin. *Cell and Tissue Research*, *285*(1), 127–139. https://doi.org/10.1007/s004410050628

Homberg, U., Reischig, T., & Stengl, M. (2003). Neural organization of the circadian system of the cockroach *Leucophaea maderae*. *Chronobiology International*, *20*(4), 577–591. https://doi.org/10.1081/CBI-120022412

Homberg, U., Würden, S., Dircksen, H., & Rao, K. R. (1991). Comparative anatomy of pigment-dispersing hormone-immunoreactive neurons in the brain of orthopteroid insects. *Cell and Tissue Research*, *266*(2), 343–357. https://doi.org/10.1007/BF00318190

Iga, M. (2016). Pigment dispersing hormone. In Y. Takei, H. Ando, & K. Tsutsui (Eds.), *Handbook of hormones* (pp. 481-e88-1). Academic Press. https://doi.org/10.1016/B978-0-12-801028-0.00088-X

Ikeno, T., Numata, H., Goto, S. G., & Shiga, S. (2014). Involvement of the brain region containing pigment-dispersing factor-immunoreactive neurons in the photoperiodic response of the bean bug, *Riptortus pedestris*. *Journal of Experimental Biology*, *217*(3), 453–462. https://doi.org/10.1242/jeb.091801

Im, S. H., & Taghert, P. H. (2010). PDF receptor expression reveals direct interactions between circadian oscillators in *Drosophila*. *The Journal of Comparative Neurology*, *518*(11), 1925–1945. https://doi.org/10.1002/cne.22311

Ito, K., Shinomiya, K., Ito, M., Armstrong, J. D., Boyan, G., Hartenstein, V., Harzsch, S., Heisenberg, M., Homberg, U., Jenett, A., Keshishian, H., Restifo, L. L., Rössler, W., Simpson, J. H., Strausfeld, N. J., Strauss, R., & Vosshall, L. B. (2014). A systematic nomenclature for the insect brain. *Neuron*, *81*(4), 755–765. https://doi.org/10.1016/j.neuron.2013.12.017

Jain, R., & Brockmann, A. (2018). Time-restricted foraging under natural light/dark condition shifts the molecular clock in the honey bee, *Apis mellifera*. *Chronobiology International*, *35*(12), 1723–1734. https://doi.org/10.1080/07420528.2018.1509867

Janssen, T., Husson, S. J., Meelkop, E., Temmerman, L., Lindemans, M., Verstraelen, K., Rademakers, S., Mertens, I., Nitabach, M., Jansen, G., & Schoofs, L. (2009). Discovery and characterization of a conserved pigment dispersing factor-like neuropeptide pathway in *Caenorhabditis elegans*. *Journal of Neurochemistry*, *111*(1), 228–241. https://doi.org/10.1111/j.1471-4159.2009.06323.x

Kay, J., Menegazzi, P., Mildner, S., Roces, F., & Helfrich-Förster, C. (2018). The circadian clock of the ant *Camponotus floridanus* is localized in dorsal and lateral neurons of the brain. *Journal of Biological Rhythms*, *33*(3), 255–271. https://doi.org/10.1177/0748730418764738

Klose, M., Duvall, L. B., Li, W., Liang, X., Ren, C., Steinbach, J. H., & Taghert, P. H. (2016). Functional PDF signaling in the *Drosophila* circadian neural circuit is gated by Ral A-dependent modulation. *Neuron*, *90*(4), 781–794. https://doi.org/10.1016/j.neuron.2016.04.002

Kobelková, A., Závodská, R., Sauman, I., Bazalová, O., & Dolezel, D. (2015). Expression of clock genes *period* and *timeless* in the central nervous system of the Mediterranean flour moth, *Ephestia kuehniella*. *Journal of Biological Rhythms*, *30*, 104-116. https://doi.org/10.1177/0748730414568430

Krupp, J. J., Billeter, J.-C., Wong, A., Choi, C., Nitabach, M. N., & Levine, J. D. (2013). Pigment-dispersing factor modulates pheromone production in clock cells that influence mating in *Drosophila*. *Neuron*, *79*(1), 54–68. https://doi.org/10.1016/j.neuron.2013.05.019

Lichtenstein, L., Grübel, K., & Spaethe, J. (2018). Opsin expression patterns coincide with photoreceptor development during pupal development in the honey bee, *Apis mellifera*. *BMC Developmental Biology*, *18*(1), 1. https://doi.org/10.1186/s12861-018-0162-8

Lin, Y., Stormo, G. D., & Taghert, P. H. (2004). The neuropeptide pigment-dispersing factor coordinates pacemaker interactions in the *Drosophila* circadian system. *Journal of Neuroscience*, *24*(36), 7951–7957. https://doi.org/10.1523/JNEUROSCI.2370-04.2004

Ludin, N. M., Rescan, M., Cheeseman, J. F., Millar, C. D., & Warman, G. R. (2012). A honey bee (*Apis mellifera*) light phase response curve. *Chronobiology International*, *29*(4), 523–526. https://doi.org/10.3109/07420528.2012.667468

Marco Antonio, D. S., & Hartfelder, K. (2017). Toward an understanding of divergent compound eye development in drones and workers of the honeybee (*Apis mellifera* L.): A correlative analysis of morphology and gene expression. *Journal of Experimental Zoology Part B: Molecular and Developmental Evolution*, *328*(1–2), 139–156. https://doi.org/10.1002/jez.b.22696

Martin, C., Hering, L., Metzendorf, N., Hormann, S., Kasten, S., Fuhrmann, S., Werckenthin, A., Herberg, F. W., Stengl, M., & Mayer, G. (2020). Analysis of pigment-dispersing factor neuropeptides and their receptor in a velvet worm. *Frontiers in Endocrinology*, *11*, 273. https://doi.org/10.3389/fendo.2020.00273

Mayer, G., Hering, L., Stosch, J. M., Stevenson, P. A., & Dircksen, H. (2015). Evolution of pigment-dispersing factor neuropeptides in panarthropoda: Insights from onychophora (velvet worms) and tardigrada (water bears). *Journal of Comparative Neurology*, *523*(13), 1865–1885. https://doi.org/10.1002/cne.23767

Moore, D., & Rankin, M. A. (1993). Light and temperature entrainment of a locomotor rhythm in honeybees. *Physiological Entomology*, *18*, 271–278. https://doi.org/10.1111/j.1365-3032.1993.tb00599.x

Moritz, R. F., & Kryger, P. (1994). Self-organization of circadian rhythms in groups of honeybees (*Apis mellifera* L.). *Behavioral Ecology and Sociobiology*, *34*(3), 211–215. https://doi.org/10.1007/BF00167746

Nässel, D. R., Shiga, S., Mohrherr, C. J., & Rao, K. R. (1993). Pigment-dispersing hormone-like peptide in the nervous system of the flies *Phormia* and *Drosophila*: Immunocytochemistry and partial characterization. *Journal of Comparative Neurology*, *331*(2), 183–198. https://doi.org/10.1002/cne.903310204

Nässel, D. R., Shiga, S., Wikstrand, E. M., & Rao, K. R. (1991). Pigment-dispersing hormone-immunoreactive neurons and their relation to serotonergic neurons in the blowfly and cockroach visual system. *Cell and Tissue Research*, *266*(3), 511–523. https://doi.org/10.1007/BF00318593

Nishiitsutsuji-Uwo, J., & Pittendrigh, C. S. (1968). Central nervous system control of circadian rhythmicity in the cockroach. *Journal of Comparative Neurology*, *58*, 14–46.

Page, T. L. (1982). Transplantation of the cockroach circadian pacemaker. *Science*, *216*(4541), 73. https://doi.org/10.1126/science.216.4541.73

Pan, Y., Zhou, Y., Guo, C., Gong, H., Gong, Z., & Liu, L. (2009). Differential roles of the fan-shaped body and the ellipsoid body in *Drosophila* visual pattern memory. *Learning & Memory*, *16*(5), 289–295. https://doi.org/10.1101/lm.1331809

Park, J. H., & Hall, J. C. (1998). Isolation and chronobiological analysis of a neuropeptide Pigment-Dispersing Factor gene in *Drosophila melanogaster*. *Journal of Biological Rhythms*, *13*(3), 219–228. https://doi.org/10.1177/074873098129000066

Petri, B., & Stengl, M. (1997). Pigment-dispersing hormone shifts the phase of the circadian pacemaker of the cockroach *Leucophaea maderae*. *Journal of Neuroscience*, *17*(11), 4087–4093. https://doi.org/10.1523/JNEUROSCI.17-11-04087.1997

Petri, B., Stengl, M., Würden, S., & Homberg, U. (1995). Immunocytochemical characterization of the accessory medulla in the cockroach *Leucophaea maderae*. *Cell and Tissue Research*, *282*(1), 3–19. https://doi.org/10.1007/BF00319128

Pfeiffer, K., & Homberg, U. (2014). Organization and functional roles of the central complex in the insect brain. *Annual Review of Entomology*, *59*(1), 165–184. https://doi.org/10.1146/annurev-ento-011613-162031

Rao, K. R., & Riehm, J. P. (1993). Pigment-dispersing hormones. *Annals of the New York Academy of Sciences*, *680*, 78–88. https://doi.org/10.1111/j.1749-6632.1993.tb19676.x

Reischig, T., Petri, B., & Stengl, M. (2004). Pigment-dispersing hormone (PDH)-immunoreactive neurons form a direct coupling pathway between the bilaterally symmetric circadian pacemakers of the cockroach *Leucophaea maderae*. *Cell and Tissue Research*, *318*(3), 553–564. https://doi.org/10.1007/s00441-004-0927-1

Reischig, T., & Stengl, M. (2002). Optic lobe commissures in a three-dimensional brain model of the cockroach *Leucophaea maderae*: A search for the circadian coupling pathways. *The Journal of Comparative Neurology*, *443*(4), 388–400. https://doi.org/10.1002/cne.10133

Reischig, T., & Stengl, M. (2003a). Ectopic transplantation of the accessory medulla restores circadian locomotor rhythms in arrhythmic cockroaches (*Leucophaea maderae*). *Journal of Experimental Biology*, *206*(11), 1877–1886. https://doi.org/10.1242/jeb.00373

Reischig, T., & Stengl, M. (2003b). Ultrastructure of pigment-dispersing hormone-immunoreactive neurons in a three-dimensional model of the accessory medulla of the cockroach *Leucophaea maderae*. *Cell and Tissue Research*, *314*(3), 421–435. https://doi.org/10.1007/s00441-003-0772-7

Renn, S. C. P., Park, J. H., Rosbash, M., Hall, J. C., & Taghert, P. H. (1999). A *pdf* neuropeptide gene mutation and ablation of PDF neurons each cause severe abnormalities of behavioral circadian rhythms in *Drosophila*. *Cell*, *99*(7), 791–802. https://doi.org/10.1016/S0092-8674(00)81676-1

Saunders, D. S., Gillanders, S. W., & Lewis, R. D. (1994). Light-pulse phase response curves for the locomotor activity rhythm in *Period* mutants of *Drosophila melanogaster*. *Journal of Insect Physiology*, *40*(11), 957–968. https://doi.org/10.1016/0022-1910(94)90134-1

Saunders, D. S., & Thomson, E. J. (1977). 'Strong' phase response curve for the circadian rhythm of locomotor activity in a cockroach (*Nauphoeta cinerea*). *Nature*, *270*(5634), 241–243. https://doi.org/10.1038/270241a0

Schendzielorz, J., & Stengl, M. (2014). Candidates for the light entrainment pathway to the circadian clock of the Madeira cockroach *Rhyparobia maderae*. *Cell and Tissue Research*, *355*(2), 447–462. https://doi.org/10.1007/s00441-013-1757-9

Schlichting, M., Menegazzi, P., Lelito, K. R., Yao, Z., Buhl, E., Dalla Benetta, E., Bahle, A., Denike, J., Hodge, J. J., Helfrich-Forster, C., & Shafer, O. T. (2016). A neural network underlying circadian entrainment and photoperiodic adjustment of sleep and activity in *Drosophila*. *Journal of Neuroscience*, *36*(35), 9084–9096. https://doi.org/10.1523/JNEUROSCI.0992-16.2016

Schneider, N.-L., & Stengl, M. (2005). Pigment-Dispersing Factor and GABA synchronize cells of the isolated circadian clock of the cockroach *Leucophaea maderae*. *The Journal of Neuroscience*, *25*(21), 5138. https://doi.org/10.1523/JNEUROSCI.5138-A-04.2005

Schulze, J., Schendzielorz, T., Neupert, S., Predel, R., & Stengl, M. (2013). Neuropeptidergic input pathways to the circadian pacemaker center of the Madeira cockroach analysed with an improved injection technique. *European Journal of Neuroscience*, *38*, 2842–2852.

Sehadová, H., Markova, E. P., Sehnal, F., & Takeda, M. (2004). Distribution of circadian clock-related proteins in the cephalic nervous system of the silkworm, *Bombyx mori*. *Journal of Biological Rhythms*, *19*(6), 466–482. https://doi.org/10.1177/0748730404269153

Selcho, M., Millán, C., Palacios-Muñoz, A., Ruf, F., Ubillo, L., Chen, J., Bergmann, G., Ito, C., Silva, V., Wegener, C., & Ewer, J. (2017). Central and peripheral clocks are coupled by a neuropeptide pathway in *Drosophila*. *Nature Communications*, *8*, 15563. https://doi.org/10.1038/ncomms15563

Shafer, O. T., & Yao, Z. (2014). Pigment-dispersing factor signaling and circadian rhythms in insect locomotor activity. *Current Opinion in Insect Science*, *1*, 73–80. https://doi.org/10.1016/j.cois.2014.05.002

Siehler, O., & Bloch, G. (2020). Colony volatiles and substrate-borne vibrations entrain circadian rhythms and are potential cues mediating social synchronization in honey bee colonies. *Journal of Biological Rhythms*, *35*(3), 246–256. https://doi.org/10.1177/0748730420913362

Siehler, O., Wang, S., & Bloch, G. (2021). Social synchronization of circadian rhythms with a focus on honeybees. *Philosophical Transactions of the Royal Society B: Biological Sciences*, *376*(1835), 20200342. https://doi.org/10.1098/rstb.2020.0342

Soehler, S., Stengl, M., & Reischig, T. (2011). Circadian pacemaker coupling by multi-peptidergic neurons in the cockroach *Leucophaea maderae*. *Cell and Tissue Research*, *343*(3), 559–577. https://doi.org/10.1007/s00441-010-1091-4

Steijven, K., Spaethe, J., Steffan-Dewenter, I., & Härtel, S. (2017). Learning performance and brain structure of artificially-reared honey bees fed with different quantities of food. *PeerJ*, *5*, e3858. https://doi.org/10.7717/peerj.3858

Stengl, M., & Arendt, A. (2016). Peptidergic circadian clock circuits in the Madeira cockroach. *Current Opinion in Neurobiology*, *41*, 44–52. https://doi.org/10.1016/j.conb.2016.07.010

Stengl, M., & Homberg, U. (1994). Pigment-dispersing hormone-immunoreactive neurons in the cockroach *Leucophaea maderae* share properties with circadian pacemaker neurons. *Journal of Comparative Physiology A*, *175*, 203–213. https://doi.org/10.1007/BF00215116

Strauss, R., & Heisenberg, M. (1993). A higher control center of locomotor behavior in the *Drosophila* brain. *The Journal of Neuroscience*, *13*(5), 1852–1861. https://doi.org/10.1523/JNEUROSCI.13-05-01852.1993

Sumiyoshi, M., Sato, S., Takeda, Y., Sumida, K., Koga, K., Itoh, T., Nakagawa, H., Shimohigashi, Y., & Shimohigashi, M. (2011). A circadian neuropeptide PDF in the honeybee, *Apis mellifera*: CDNA cloning and expression of mRNA. *Zoological Science*, *28*(12), 897–909. https://doi.org/10.2108/zsj.28.897

Sun, B., & Salvaterra, P. M. (1995). Characterization of nervana, a *Drosophila melanogaster* neuron-specific glycoprotein antigen recognized by anti-horseradish peroxidase antibodies. *Journal of Neurochemistry*, *65*(1), 434–443. https://doi.org/10.1046/j.1471-4159.1995.65010434.x

Talsma, A. D., Christov, C. P., Terriente-Felix, A., Linneweber, G. A., Perea, D., Wayland, M., Shafer, O. T., & Miguel-Aliaga, I. (2012). Remote control of renal physiology by the intestinal neuropeptide pigment-dispersing factor in Drosophila. *Proceedings of the National Academy of Sciences*, *109*(30), 12177–12182. https://doi.org/10.1073/pnas.1200247109

Tomioka, K., Miyasako, Y., & Umezaki, Y. (2008). PDF as a coupling mediator between the light-entrainable and temperature-entrainable clocks in *Drosophila melanogaster*. *Acta Biologica Hungarica*, *59*(Suppl 2), 149–155. https://doi.org/10.1556/ABiol.59.2008.Suppl.23

Tweedy, D. G., & Stephen, W. P. (1970). Light refractive emergence rhythm in leafcutter bee, *Megachile rotundata* (F.) (Hymenoptera: Apoidea).

Cellular and Molecular Life Sciences, *26*(4), 377–379. https://doi.org/10.1007/BF01896898

Vafopoulou, X., Terry, K. L., & Steel, C. G. H. (2009). The circadian timing system in the brain of the fifth larval instar of *Rhodnius prolixus* (Hemiptera). *The Journal of Comparative Neurology*, *518*, 1264–1282. https://doi.org/10.1002/cne.22274

von Frisch, K. (1967). *Dance language and orientation of bees*. Harvards University Press.

Wei, H., el Jundi, B., Homberg, U., & Stengl, M. (2010). Implementation of pigment-dispersing factor-immunoreactive neurons in a standardized atlas of the brain of the cockroach *Leucophaea maderae*. *The Journal of Comparative Neurology*, *518*(20), 4113–4133. https://doi.org/10.1002/cne.22471

Wei, H., Yasar, H., Funk, N. W., Giese, M., Baz, E.-S., & Stengl, M. (2014). Signaling of Pigment-Dispersing Factor (PDF) in the Madeira cockroach *Rhyparobia maderae*. *Plos One*, *9*(9), e108757. https://doi.org/10.1371/journal.pone.0108757

Weiss, R., Dov, A., Fahrbach, S. E., & Bloch, G. (2009). Body size-related variation in pigment dispersing factor-immunoreactivity in the brain of the bumblebee *Bombus terrestris* (Hymenoptera, Apidae). *Journal of Insect Physiology*, *55*(5), 479–487. https://doi.org/10.1016/j.jinsphys.2009.01.016

Wise, S., Davis, N. T., Tyndale, E., Noveral, J., Folwell, M. G., Bedian, V., Emery, I. F., & Siwicki, K. K. (2002). Neuroanatomical studies of *period* gene expression in the hawkmoth,*Manduca sexta*. *The Journal of Comparative Neurology*, *447*(4), 366–380. https://doi.org/10.1002/cne.10242

Yao, Z., & Shafer, O. T. (2014). The *Drosophila* circadian clock is a variably coupled network of multiple peptidergic units. *Science*, *343*(6178), 1516–1520. https://doi.org/10.1126/science.1251285

Yasuyama, K., & Meinertzhagen, I. A. (1999). Extraretinal photoreceptors at the compound eye's posterior margin in *Drosophila* melanogaster. *Journal of Comparative Neurology*, *412*(2), 193–202. https://doi.org/10.1002/(SICI)1096-9861(19990920)412:2%3c193::AID-CNE1%3e3.0.CO;2-0

Závodská, R., Šauman, I., & Sehnal, F. (2003). Distribution of PER protein, pigment-dispersing hormone, prothoracicotropic hormone, and eclosion hormone in the cephalic nervous system of insects. *Journal of Biological Rhythms*, *18*(2), 106–122. https://doi.org/10.1177/0748730403251711

Zeller, M., Held, M., Bender, J., Berz, A., Heinloth, T., Hellfritz, T., & Pfeiffer, K. (2015). Transmedulla neurons in the sky compass network of the honeybee (*Apis mellifera*) are a possible site of circadian input. *Plos One*, *10*(12), e0143244. https://doi.org/10.1371/journal.pone.0143244

How to cite this article: Beer, K., Härtel, S., & Helfrich-Förstерm, C. (2022). The pigment-dispersing factor neuronal network systematically grows in developing honey bees. *Journal of Comparative Neurology*, *530(9)*, 1321–1340. https://doi.org/10.1002/cne.25278